This manuscript is under submission with "JOURNAL OF ASIAN EARTH SCIENCES".

Detrital zircon U-Pb ages of Proterozoic and Cretaceous sandstones of Narmada region in Central India: Implications for provenance and the closure age of the Vindhyan Basin

Vandana Kumari[a], Sampat Kumar Tandon[a], J Kallukalam Tomson[b,*], Arundhuti Ghatak[a,c,*]

[a]Department of Earth and Environmental Sciences, Indian Institute of Science Education and Research Bhopal, Bhopal Bypass Road, Bhauri, Bhopal, 462066, Madhya Pradesh, India.

[b]National Centre for Earth Science Studies, Thiruvananthapuram, 695011, Kerala, India.

[c]Centre for Research on Environment and Sustainable Technologies, Indian Institute of Science Education and Research Bhopal, Bhopal Bypass Road, Bhauri, Bhopal, 462066, Madhya Pradesh, India.

*Corresponding Author: arundhutighatak@iiserb.ac.in, tomson.jk@ncess.gov.in

Abstract

This study presents detrital zircon U-Pb ages of the Upper Bhander Sandstones from the Bhopal inlier, and the overlying Cretaceous sandstones from Jabalpur, Central India. These data are combined with existing palaeobiological evidence to address the issue of lack of convergence between geochronology and biochronology of the Upper Vindhyan succession in central India. The age-spectra of Upper Bhander Sandstone show the dominance of detrital zircon population between 1500-1900 Ma, a subordinate cluster of 2400-2600 Ma, and a single youngest zircon grain of ~770 Ma. These detrital zircon ages correlate with the timing of granite magmatism in Bundelkhand, Aravalli and Central Indian Tectonic Zone (CITZ), implying their derivation from these terranes. The finding of a single zircon of 770 $\pm$ 12 Ma, supports the premise that Vindhyan deposition extended in to the late Tonian. Cretaceous sandstones of the Jabalpur and Lameta Formations contain zircon grains of ~550 Ma and ~700-800 Ma age. Except for the evidence from this youngest Vindhyan sedimentary sequence, no rocks of Late Neoproterozoic-Early Cambrian age have so far been reported from Central India, which can be correlated with these zircon ages. Comparable age-spectra of the Upper Bhander and the Cretaceous sandstones indicates that the proximal Vindhyan sandstones could have supplied detritus to these younger sandstones. These Cretaceous sandstones also constitute a window to understand the geology of the pre-Cretaceous eroded terrain, and support the premise that the Vindhyan sedimentation did not terminate at 1000 Ma.

Keywords: Bhopal Vindhyan inlier; Detrital Zircons; Tonian; Upper Bhander Sandstone; Vindhyan Basin

1. Introduction

Proterozoic supercontinent cycles played a pivotal role in shaping the Indian subcontinent and largely controlled the development and evolution of the exceptionally well preserved ‘Purana’ basins (Meert et al., 2010; Meert and Pandit, 2015; Wang et al., 2021). Some of these 'Purana' basins of the Indian subcontinent are hosted by the Archean craton dominated landmass composed of the Banded Gneissic Complex, Bundelkhand, Bastar, and Singhbhum cratons separated by Aravalli Delhi Fold Belt (ADFB) and Central Indian Tectonic Zone (CITZ) (Fig. 1A-B; Basu and Bickford, 2015; Chakraborty et al., 2020; Kaur et al., 2022; Meert and Pandit, 2015; Wang et al., 2019). These Proterozoic sedimentary packages covering different parts of peninsular India provide a window into the tectonic, biological and climatic evolution and near surface processes of almost a billion years of Earth history during the Proterozoic (Chakraborty et al., 2020). The Vindhyan basin, one of the largest Proterozoic basins in the world, evolved in response to the breakup of Columbia and the amalgamation of Rodinia supercontinents (Fig. 1A-B; Basu and Bickford, 2015). It hosts the thickest Proterozoic sedimentary succession of the Indian subcontinent, referred to as the 'Vindhyan Supergroup'. The Lower Vindhyan (Semri Group) and the Upper Vindhyan (Kaimur, Rewa and Bhander Groups) successions have been extensively studied in terms of palaeobiology (Azmi, 1998, Azmi et al., 2008; Bengtson et al., 2009; Bengtson et al., 2017; De 2003, 2006; Kumar and Pandey, 2008; Kumar and Sharma, 2012; Kumar and Srivastava, 2003; Retallack et al., 2021; Seilacher et al., 1998; Sharma, 2006; Sharma and Shukla, 2009a, 2009b; Srivastava, 2002, 2011, 2012) and geochronology (Bickford et al., 2017; Colleps et al., 2021; George et al., 2018; Gilleaudeau et al., 2018; Gopalan et al., 2013; Kumar et al., 2001; Kumar et al., 2002; Lan et al., 2020, 2021; Malone et al., 2008; McKenzie et al., 2011; Mishra et al., 2018; Rasmussen et al., 2002; Ray et al., 2002, 2003; Ray, 2006; Sarangi et al., 2004; Tripathy and Singh, 2015; Turner et al., 2014) to constrain their depositional ages. Robust geochronological constraints based on zircon ages of the tuffaceous unit of Semri Group (Fig. 2; Bickford et al., 2017; Rasmussen et al., 2002; Mishra et al., 2018; Ray et al., 2002), and ages of the basal limestone bed (Kajrahat limestone; 1729 ± 110 Ma), and a limestone (Rohtas limestone; 1599 ± 48 Ma) from the top of the Semri Group (Sarangi et al., 2004) suggest an initiation age of 1750 Ma for the Vindhyan Basin. Although the Lower Vindhyan (Semri Group) is geochronologically well constrained, the Upper Vindhyan succession lacks robust age constraints due to the absence of volcanic tuffaceous/pyroclastic materials (e.g., Tripathy and Singh, 2015). However, detrital zircon geochronological data from the Upper Vindhyan sandstones are available and generally show a lack of zircons younger than 1000 Ma, evidence that has served as a pointer to the closure of the Vindhyan Basin at ~1000 Ma (Chakraborty et al, 2020; Malone et al., 2008; McKenzie et al., 2011; Turner et al., 2014). Additionally, paleomagnetic evidence has also been used to suggest the termination of Vindhyan sedimentation at the end of the Mesoproterozoic (Malone et al., 2008; Meert et al., 2013; Turner et al., 2014; Venkateshwarlu and Rao; 2013). In contrast to detrital zircon geochronology, other radiometric dates such as Pb-Pb and Sr-isotopic ages suggest that the deposition of the Upper Vindhyan succession continued until at least ~800 Ma (George et al., 2018; Gopalan et al., 2013; Ray et al., 2003; Srivastava and Rajagopalan, 1988). Additionally, some of the palaeobiological evidence suggests an Ediacaran age for the deposition of the Bhander Group, the youngest unit of the Upper Vindhyan Group (De, 2006; Kumar and Pandey, 2008). In view of the lack of convergence between geochronology and biochronology of the Upper Vindhyan succession, further investigations are required to resolve the age of closure of the basin.

The recent mistaken identification of the Ediacaran fossil '*Dickinsonia*' from the Upper Bhander Sandstone at Bhimbetka near Bhopal, Madhya Pradesh (M.P.) by Retallack et al (2021) and its recognition later as extant beehive impressions (Meert et al., 2023) together with the occurrence of a single youngest ~548 Ma zircon grain from the Maihar Sandstone at Maihar (M.P.) (Lan et al., 2020) has raised interest on the re-assessment of the closure age of the Vindhyan basin. Recent work by Pandey et al (2023) have also convincingly shown that the *Dickonsonia* reported by Retallack et al (2021) is related to extant fallen beehives, and should therefore be placed in the category of a pseudofossil. Here, we present, for the first time, U-Pb detrital zircon geochronology of the Upper Bhander Sandstone exposed in the Bhopal inlier. Additionally, new detrital zircon U-Pb ages have also been presented for the stratigraphically younger Cretaceous sandstones of the Jabalpur and Lameta Formations, exposed in Jabalpur region of Central India. These younger clastic sedimentary rocks of the Cretaceous provide insights into the pre-Cretaceous provenance, as well as additional data to explore the age discrepancy of the Upper Vindhyan. We integrated zircon age data with our petrographic and geochemical data along with the published paleocurrent data (e.g., Akhtar, 1978; Ansari, 1994; Bhattacharya and Morad, 1993; 1996; Chanda and Bhattacharya, 1966; Raza and Casshyap) to provide an improved understanding of the provenance for these Proterozoic and Cretaceous sandstones.

2. Geological background

2.1. The Vindhyan basin

The Vindhyan basin is a large intracratonic basin filled with unmetamorphosed and mildly deformed Proterozoic sedimentary rocks (Bose et al., 2001). It is an arcuate basin developed in the central part of the Indian shield, bounded in the west by the ADFB and in the south and southeast by CITZ (Fig. 1 A-B; Chakrabarti et al., 2007; Chakraborty, 2006; Ramakrishnan and Vaidyanadhan, 2010). Low-grade metamorphic rocks of the Mahakoshal Group form the eastern margin of the basin, whereas it is bordered by recent alluvium in the north, and covered by Deccan lavas in the south (Fig. 1B; Chakrabarti et al., 2007; Chakraborty, 2006; Ramakrishnan and Vaidyanadhan, 2010). The Bundelkhand massif divides the Vindhyan Basin into the Son Valley sector and the Chambal Valley sector or the Rajasthan sector (Kumar, 2012; Valdiya, 2016). It has been suggested that siliciclastic rocks exposed in both these sectors received sediments from different sources (Chakrabarti et al., 2007). The rocks of the Vindhyan

Supergroup are stratigraphically divided into four Groups: Semri, Kaimur, Rewa and Bhander (Fig. 1B, 2). The presence of a pronounced regional unconformity at the base of the Kaimur Group divides the succession into the Lower Vindhyan and the Upper Vindhyan (Kale et al., 2016; Kumar, 2012; Valdiya, 2016). The Semri Group forms the lower part of the Vindhyan Supergroup, which comprises five formations in the Son Valley sector i.e., Deoland, Kajrahat, Porcellanite (Deonar Formation), Kheinjua, and Rohtas, in order of superposition (Fig. 2A). The Upper Vindhyan is constituted by the Kaimur, Rewa and Bhander groups in ascending order (Fig. 2). The Vindhyan basin is characterised by ~5000m thick succession composed of sandstone, shale, conglomerate and carbonate with subordinate felsic volcanics. The depositional environment for the Vindhyan sediments ranges from continental (alluvial fan) to marine shelf (tidal flat to storm dominated shelf) (Bose et al., 2001).

The Lower Vindhyan succession (Semri Group) is composed predominantly of carbonates and shales with subordinate sandstone and volcaniclastic materials, and deposited mainly in shelf and shallow marine environments (Bose et al., 2001). The Semri Group is up to 1.7 km thick (Soni et al.,1987), and is unconformably deposited on a basement of 2492±10 Ma Bundelkhand granites (Mondal et al., 2002) or 1854±7 Ma Hindoli Group (Deb et al., 2001). Occurrence of carbonate sequences such as Kajrahat, Salkhan and Rohtas limestone as well as volcaniclastic materials in the Porcellanite Formation, enables determination of absolute age of the Lower Vindhyan succession. Based on several radiometric data such as U-Pb zircon ages of volcanic tuffs and rhyolite (Rasmussen et al., 2002; Ray et al., 2002; Bickford et al., 2017) and Pb-Pb ages of carbonates (Ray, 2006; Sarangi et al., 2004), the age of the lower Vindhyan succession has been reliably constrained between ~1750-1500 Ma (Fig. 2).

2.2. Debate on the termination age of Upper Vindhyan sedimentation

Due to the absence of volcanic tuffaceous material in the Upper Vindhyan succession, detrital zircon U-Pb geochronology has been applied to constrain its maximum depositional age. This, in turn, can provide critical constraints on the timing of closure of the Upper Vindhyan succession. U–Pb concordia dates of the youngest detrital zircons within the Upper Bhander Sandstone unit of the Upper Vindhyan, constrain its maximum depositional age to ~1020 Ma (Malone et al., 2008). Several studies argue for a Late Mesoproterozoic to Early Neoproterozoic age for the Upper Vindhyan based on palaeomagnetic studies and the general absence of zircon grains younger than ~1000 Ma in the Upper Vindhyan succession (Fig. 2; Malone et al., 2008; McKenzie et al., 2011; Turner et al., 2014; Chakraborty et al., 2020). However, Kumar et al. (2002) proposed a 700-570 Ma age range for the Bhander Group on the basis of oxygen, carbon and strontium isotopic signatures. Based on Sr isotope stratigraphy of carbonates from the Upper Vindhyan (Son Valley sector) a Mid-Neoproterozoic age (~750 Ma) has also been suggested for the Bhander Group (Fig. 2; Ray, 2003). Strontium isotope stratigraphy and $\delta^{13}C$ shift in the Balwan limestone (Fig. 2) together with their Pb-Pb age (866 ± 90 Ma), present strong evidence for the continuation of Upper Vindhyan sedimentation during the Tonian Period (Fig. 2; George et al., 2018; Gopalan et al., 2013). Recently, Lan et al., (2020) reported a youngest detrital zircon of 548 Ma age from the Maihar Sandstone (Fig. 2); however, also see Bickford and Basu (2021) for different views. From these multiple data sets, it is observed that there is no consistency in the stratigraphic ages proposed by different authors. Notably, the geochronology also shows divergence from the ages proposed on the basis of palaeobiologic evidence. The presence of *Arumberia* and other Ediacaran-like fossils suggests an Ediacaran age as the upper limit of the Vindhyan sedimentation (Kumar and Pandey, 2008, De 2006).

2.3. Upper Bhander Sandstone (equivalent to Maihar Sandstone) from Bhopal inlier

Sandstones exposed in the Bhopal inlier including Bhimbetka belong to the Upper Bhander Sandstone (Bhander Group) of the Vindhyan Supergroup (Fig. 3A-C; Retallack et al., 2021). The equivalent Maihar Sandstone in its type area, composed of sandstone, siltstone and subordinate shale, is considered to be the youngest stratigraphic horizon of the Bhander Group, showing gradational contact with the underlying Sirbu Shale. The Upper Bhander Sandstones in and around Bhopal occur as isolated outcrops forming the southwestern part of the Vindhyan Basin (Fig. 3A; Mohammadi et al., 2014; Mohammadi, 2015). They are primarily red colored sandstones that are interbedded with yellow/brown siltstone (Fig. 3D). These ferruginous and non-calcareous sandstone beds dip northward at ~10 degrees. Planar bedding is the most prominently developed sedimentary structure in the Bhimbetka Sandstone (Fig. 3D). Structures such as ripple marks and trough cross bedding are also observed at some places.

2.4. Cretaceous sandstones from Jabalpur, Central India

Jabalpur and neighboring areas located in the CITZ have a stratigraphic record ranging from Precambrian to the Mesozoic (Fig. 4A-B). In this region, the meta-sedimentary sequences of the Mahakoshal Group are intruded by Madan Mahal Granites, and constitute the Precambrian basement (Fig. 4B-C; Yadav et al., 2020). The Proterozoic Vindhyan sedimentary rocks occur in this region with extensive development of the Bhander Group (Fig. 4C). Sedimentation of the Early Cretaceous rocks of Jabalpur Formation (Upper Gondwana) and the Late Cretaceous Lameta Formation commenced, following a pronounced hiatus after the deposition of the Vindhyan sediments (Fig. 4B-C). The Lameta Formation is overlain by Deccan lava flows (Tandon, 2002). As these Cretaceous rocks rest on the Precambrian basement in Jabalpur region, the zircon population of these younger sediments should have preserved the geologic imprints of the older eroded terrains (Mahakoshal and Vindhyan Supergroup) of the region. These younger sedimentary sequences can therefore provide a window into the geology of the pre-Cretaceous eroded terrain and allow a comparison of the sources for the Neoproterozoic and Cretaceous sandstones.

2.4.1. Jabalpur (White) Sandstone from Early Cretaceous Jabalpur Formation

The rocks of the Jabalpur Formation constitute the topmost part of the Gondwana sequence and unconformably overlie the Precambrian rocks in their type area (Fig. 4B-C). The Jabalpur Formation derived its name from Jabalpur city where it has an exposed thickness of ~16 m in a quarry (Chhui Hill section) near the railway station (Fig. 5A). It consists of white to brown cross bedded sandstones alternating with white clays (Fig. 5A; Chanda and Bhattacharya, 1966; Dogra et al., 1994). Sedimentation took place in fluvial conditions which is evident from the fining upward sequence, palynofloral assemblage, and a lack of phytoplankton and coastal vegetation (Dogra et al., 1994). Paleocurrent data from the cross-bedded sandstones indicates its deposition by southerly to southwesterly flowing rivers (Fig. 5; Chanda and Bhattacharya, 1966). Systematic field investigation and stratigraphy, coupled with palynological evidence indicates a Late Jurassic-Early Cretaceous (Tithonian-Neocomian) age for the Jabalpur Formation (Dogra et al., 2010).

2.4.2. Green Sandstone and Upper Calcified Sandstone from Late Maastrichtian Lameta Formation

The Lameta Formation is composed of arenaceous, argillaceous and calcareous facies, and is overlain by Deccan basalts. This Formation occurs in discontinuous patches along the Narmada Valley in central India due to the non-uniform erosion of overlying Deccan basalts as well as their deposition in localized terrestrial settings (Tandon et al., 1995). Green Sandstone constitutes the basal part of the Maastrichtian Lameta Formation (Fig. 5). It unconformably overlies the Jabalpur clay in the Chhui Hill area, Jabalpur (Fig. 5A). It consists of medium to coarse grained sandstones which commonly show trough cross stratification (Fig. 5B). These sandstones show a conspicuous green colour due to the presence of smectite group of clays and celadonite (e.g., Tandon et al., 1995). Green Sandstone is deposited by southwest directed shallow, braided and ephemeral channels (Fig. 5; Tandon et al., 1995).

The Upper Calcified Sandstone is the uppermost unit of the Lameta Formation with a uniform thickness (<5 m), and is overlain by Deccan Basalts in the Jabalpur region (Fig. 5; Tandon et al., 1995). It is a poorly to moderately sorted indurated sandstone which has been extensively calcified (Fig. 5C; Tandon et al., 1995). It contains pebbles of jasper and chert along with abundant green mud clasts. These are dominantly trough cross-bedded sandstones deposited by northeast directed unchanneled sheetflows (Fig. 5; Tandon et al., 1995).

3. Sampling and analytical methods

A total of seven sandstone samples (3-5 kg each) were collected for detrital zircon U-Pb analyses, out of which four samples are from the Upper Bhander Sandstone exposed in Bhopal and Bhimbetka (Southeast of Bhopal) area (Fig. 3A-C) and the other three samples are of the stratigraphically younger sandstones exposed in Jabalpur (Fig. 4A, C). These younger sandstones exposed in between Bhimbetka and Maihar area are chosen to obtain insights into the geological history of the older Precambrian eroded terrain (Fig. 4A, C).

The samples were powdered to ~200 mesh for whole rock geochemical analysis. Powdered samples were weighed with a mixture of 1:1 lithium tetraborate and metaborate flux in a platinum (Pt) crucible to make fused glass beads. Major element compositions of fused bead samples were determined using ED-XRF at the Earth and Environmental Sciences laboratory of IISER Bhopal. Certified Reference Materials (CRMs) from USGS such as BIR-1 (Icelandic Basalt), BCR-2 (Basalt, Columbia River); RGM-2 (Rhyolite, Glass Mountain) and SGR-1b (Green River Shale) were used for calibration and also run as unknown standards to check the data quality. The analytical uncertainties were <10% for all the samples. Trace element analysis of bulk samples was carried out using a Thermo iCAP-q quadrupole ICP-MS at Department of Earth and Environmental Sciences, IISER Bhopal. For measurement of trace element concentration of bulk sample, 25 mg of the samples were accurately weighed and digested following the closed vessel acid digestion method with a mixture of HF and HNO_3, and heated up to 120°C for 48 hours. The dried sample was acidified in HNO_3 (2%) and diluted 4000 times. The standards and samples were spiked with 10 ppb internal standard (In, Cs, Re, and Bi) for trace element measurements. USGS rock standards namely BCR-2 (Basalt, Columbia River), BHVO-2 (Hawaiian Basalt), BIR-1 (Icelandic Basalt) AGV-2 (Guano Valley Andesite), RGM-2 (Rhyolite, Glass Mountain), GSP-2 (Granodiorite, Silver Plume, Colorado), and SGR-1b (Green River Shale) were used for calibration and also run as control standards to check the accuracy. Procedural blanks were prepared and run for each batch of samples during analyses. The analytical uncertainty was <5% for the trace elements and <2% for rare earth elements.

Detrital zircons were separated from the bulk rock using conventional Wilfley table and Franz LB1-magnetic barrier techniques at the thin section and sample preparation laboratory at National Centre for Earth Science Studies (NCESS), Thiruvananthapuram. Individual zircon grains were handpicked, and mounted on a 25 mm epoxy disc. The grains range in size between 50 to 300 microns. The epoxy discs are further ground and polished to expose the internal structures of mounted grains. Back scattered electron (BSE) and cathodoluminescence (CL) imaging of zircons were performed using CAMECA SX Five Tactics Electron Probe Microanalyzer (EPMA) and TESCAN Vega 4 Scanning electron microscope (SEM) at NCESS. Zircon U-Pb isotope and trace element analysis were carried out using Teledyne CETAC, Nd:YAG (213nm) laser ablation system coupled with Agilent 7800 quadrupole ICPMS, housed at the Isotope Geochemistry Facility (IGF), NCESS. The detailed analytical protocol is according to Dev et al., 2021. Approximately 100 zircon grains from each sample were analysed for U-Pb isotopes whereas trace element analysis on zircons was performed only for the Upper Bhander Sandstone (Bhimbetka). Zircon grains were analysed at a spot size of 30 µm at 10Hz repetition rate in Q-switch mode. The '91500 zircon' (Wiedenbeck et al., 1995) was used as the primary reference material for U-Pb geochronology whereas Plešovice ($^{206}Pb/^{238}U$ age of 337.13 ± 0.37 Ma; Sláma et al., 2008) and BB11 zircon standards ($^{206}Pb/^{238}U$ age of 560 ± 1.1 Ma; Santos et al., 2017) were analyzed as unknowns for quality control. During the analytical session, Plešovice and BB-11 zircon standard yielded a weighted mean $^{206}Pb/^{238}U$ age of 337.9 ± 2.5 Ma and 571.1 ± 3.1 Ma respectively, well within the reported error limit. For zircon trace element analysis, NIST 610 (Pearce et al., 1997) was used as primary reference standard whereas ^{29}Si (IS value=14.78) was used as the internal standard. Data processing were carried out offline using the Iolite 4.4 (Paton et al., 2011) with the integrated Visual Age Package (Petrus and Kamber, 2012). Concordia diagrams and probability density plots with histograms were made using Isoplot (version 4.15, Ludwig, 2012). All errors on ratios and ages are reported at 2σ confidence level. Grains with discordance values of <10 % were chosen to plot probability density curves and concordia diagrams. The choice of "best age" is as per the method outlined in Spencer et al. (2016), where $^{207}Pb/^{206}Pb$ ages are reported for grains older than 1000 Ma while $^{206}Pb/^{238}U$ ages are reported for zircons younger than 1000 Ma. All chondrite normalizations are according to Taylor and McLennan, (1985).

4. Results

4.1. Petrographic study

4.1.1. Upper Bhander Sandstone from the Bhopal inlier

The sandstone is composed of quartz, subordinate feldspar, and lithic fragments with mica, tourmaline and zircon as accessory minerals (Fig. 6A-C). Subangular to subrounded quartz grains constitute the major portion (~90%) of the sandstone, and sometimes exhibit iron oxide coatings. Monocrystalline quartz dominates over the polycrystalline quartz grains. Potassium feldspar is the second major constituent of the rock and accounts for about 5% of the bulk sample, followed by lithic fragments (quartzite, chert) which comprise nearly 3% of the sample

(Fig. 6A-B). Grains are compacted showing concavo-convex boundaries. Petrographic investigations reveal that the sandstone is medium to fine grained, moderate to well-sorted quartz arenite, with a high degree of compositional and textural maturity (Fig. 6A-C). The presence of polycrystalline and undulated quartz grains indicates metamorphic rocks as one of the possible sources for these sandstones.

4.1.2. Cretaceous Sandstones of Jabalpur

4.1.2.1. Jabalpur (White) Sandstone from the Jabalpur Formation

The white sandstone is medium to fine grained, moderately sorted, with quartz, K-feldspar and mica as primary framework constituents (Fig. 5A). Quartz grains floating in a micaceous matrix are angular to subangular in shape. The sandstone is texturally submature but it shows mineralogical maturity with lesser proportions of feldspars as compared to quartz. Clayey matrix and ferruginous cements are also present in traces.

4.1.2.2. Green Sandstone and Upper Calcified Sandstone from the Lameta Formation

Framework grains of the Green Sandstone are composed mainly of quartz, feldspar and accessory minerals. The sandstone consists predominantly of quartz grains of variable shapes ranging from subangular to subrounded (Fig. 5C). Wide variation in size of the grains from silt to coarse sand size indicates poor sorting in the sandstone. Monocrystalline as well as polycrystalline quartz grains are present, the latter being more predominant. Grain-to-grain contact is absent and the interstitial spaces between the skeletal grains are filled with green clays. Montmorillonite, celadonite and kaolinite constitute the clay fraction of the sandstone (Tandon et al., 1995).

In Upper Calcified Sandstone, the framework grains are dominantly quartz with a minor amount of feldspar and mica. Large variation in size and shape of quartz grains is observed which indicates poor sorting and textural immaturity (Fig. 5D). Grain-to-grain contact is completely lost, and the detrital grains are floating in a micritic groundmass. Presence of circum-granular cracks around the skeletal grains and clay coatings on the framework grains have been noted (Fig. 5D).

4.2. Whole rock geochemistry

4.2.1. Major and trace element analyses of Upper Bhander sandstone of Bhopal inlier

These sandstones show high concentration of SiO_2 ranging from 73.9 to 88.2 wt. %. High SiO_2 content accords well with the abundance of quartz in these sandstones. The samples exhibit moderate amount of Al_2O_3 (4.3 to 7.4 wt. %) and Fe_2O_3 (2.4 to 9.1 wt. %), and very low amount of TiO_2, MnO, CaO, K_2O, Na_2O and P_2O_5. The K_2O/Na_2O ratio is greater than 1 indicating the dominance of potash feldspar over plagioclase feldspar and is also consistent with the petrographic observations. The Chondrite normalized REE pattern of these sandstones shows LREE enrichment, with La_N/Sm_N ranging from 3.13 to 4.48 and flat HREE pattern with Gd_N/Yb_N value in the range of 0.99-1.72 (Fig. 7A). All the samples show a prominent negative Eu anomaly which ranges from 0.35 to 0.59 (Fig. 7A). The LREE enriched pattern with negative Eu anomaly and very high La/Yb ratio (9.7 to 16.2) suggests the cratonic environment and most likely a felsic source for these sandstones.

The discriminant diagram proposed by Roser and Korsch (1988) is used to discriminate among felsic igneous, quartzose sedimentary, intermediate and mafic igneous provenances. All the samples fall in the field of quartzose sedimentary provenance indicating recycled granitic/gneissic or sedimentary source (Fig. 7C). Index of Compositional Variability (ICV; Cox et al., 1995) was calculated for the samples to understand their compositional maturity. ICV for Upper Bhander sandstones is close to 1 (0.9 to1.2; Fig. 7D), which suggests that these sandstones are compositionally mature and possibly deposited in tectonically stable/cratonic environments where sediment recycling was prominent. Recycling can also be confirmed by Zr/Sc versus Th/Sc plot (McLennan et al., 1993) for these samples. First-cycle sediments generally show good correlation between these ratios whereas recycled sediments are characterised by very high Zr/Sc as compared to Th/Sc ratio (Fig. 7E). The La/Sc versus Co/Th plot shows that the samples fall in the common field of TTG of Bundelkhand Craton and the rocks of Mahakoshal belt (Fig. 7F). It can be inferred that these sedimentary rocks may have been derived from the older crust (TTG) and the metasedimentary and granitic rocks (e.g., Madan Mahal) of Mahakoshal belt exposed in the surrounding terrain (Fig. 7F).

4.2.2. Major and trace element analyses of Cretaceous sandstones of Jabalpur.

As the Upper Calcified Sandstone has been diagenetically modified through calcretization, the fine-grained sandstones of the underlying Mottled Nodular Beds have been used for the bulk chemical analysis. The major element data of these sandstones indicate higher SiO_2 content (74.3 to 80.9 wt. %), moderate Al_2O_3 (2.62 to 9.22 wt. %) and low to very low content of other oxides like Fe_2O_3, TiO_2, MnO, CaO, K_2O, Na_2O and P_2O_5. REE pattern of these sandstones characterised by LREE enrichment (La_N/Sm_N = 3.98), nearly flat HREE pattern and negative Eu anomaly (0.50 to 0.65) is indicative of a felsic source for these sediments (Fig. 7B). Discrimination diagram proposed by Roser and Korsch (1988) suggests that all the samples lie within the quartzose sedimentary provenance which indicates that these sandstones may have been derived from mature polycyclic continental sedimentary source or from weathered granite gneiss (Fig. 7C). All the samples have ICV value, ranging from 0.41 to 1.09 (Fig. 7D). Based on the ICV, it can be inferred that these sandstones are compositionally mature as opposed to the first cycle deposits, and probably deposited in tectonically stable/cratonic environments through recycling (Cox et al., 1995). In Th/Sc versus Zr/Sc plot after McLennan et al. (1993), samples plot along a trend suggesting enrichment in the Zr concentration due to recycling and sorting (Fig. 7E). The La/Sc versus Co/Th plot indicates that the TTG of Bundelkhand Craton, metasedimentary rocks of Mahakoshal belt and nearby Upper Vindhyan rocks can be the possible sources for these younger sandstones (Fig. 7F).

4.3. Detrital zircon geochronology and trace element analysis of zircons from the Upper Bhander Sandstone of Bhopal and Bhimbetka, Central India

4.3.1. Detrital zircon geochronology

A total of 227 zircons were analyzed from the Upper Bhander sandstone at Bhimbetka, of which 176 grains provided concordant ages (<10% discordance) and have been used for provenance and age interpretation. Zircon grains of the Bhimbetka sandstone are subangular to subrounded in shape and range in size from 50 to 200 μm. Cathodoluminescence (CL) images show some oscillatory zoned zircon crystals. Representative CL images of grains with their concordant ages are shown in Fig. 8D. Near-concordant ages have been plotted in the Wetherill concordia diagram which shows several age clusters (Fig. 8A). Age distribution of the sample is shown in a probability density plot (Fig. 8B). The sample has the most dominant population of detrital zircons between the age interval of 1400 Ma to 1800 Ma, with a primary peak at 1740 Ma and a secondary peak at 1510 Ma. Another prominent peak at ~2470 Ma is also recorded. One Paleo-archean zircon grain is present with a $^{207}Pb/^{206}Pb$ age of 3340±47 Ma. A small cluster of zircon grains occurs in the interval of 2150-2000 Ma with a subordinate peak at 2044 Ma. A few grains reveal ages in the interval of 1000-1300 Ma, with a peak age at 1220 Ma. The youngest grain in the sample has the $^{206}Pb/^{238}U$ age of 770±12 Ma. This particular grain exhibits a high degree of concordance (~95%); therefore, the age can be considered to be robust.

Additionally, a total of 179 zircons were analyzed from Upper Bhander sandstone exposed in and around Bhopal city, of which 161 grains provided concordant ages (<10% discordance) and have been used for provenance and age interpretation. Zircon grains of these sandstones are also subangular to subrounded in shape and range in size from 50 to 200 μm. Near-concordant ages have been plotted in the Wetherill concordia diagram which shows several age clusters (Fig. 9A). Age distribution of the sample is shown in a probability density plot (Fig.

9B). The sample has the most dominant population of detrital zircons between the age interval of 1400 Ma to 1800 Ma, with a primary peak at 1730 Ma and a secondary peak at 1460 Ma. Another subordinate peak at ~2046 Ma is also recorded from these sandstones. One relatively older zircon grain is present with a $^{207}Pb/^{206}Pb$ age of 2490±116 Ma. A few grains reveal ages in the interval of 1000-1300 Ma. Overall, the detrital zircon geochronology of the Upper Bhander sandstone from the Bhopal inlier (Bhopal city and Bhimbetka collectively) suggests that the grains cluster predominantly around ~1740 Ma, and ~1500 Ma.

4.3.2. Trace element analysis of zircons

The sample has U content ranging from 42 to 1021 ppm with Th/U ratios varying from 0.16 to 2.31 with an average of 0.81 (Fig. 8C). The CL images of the grains coupled with their Th/U ratio suggests a magmatic origin for these detrital zircons. The total REE content of the zircon grains varies from 69 ppm to 17,845 ppm with an average value of 2,066 ppm. Majority of the grains exhibit a uniform Chondrite-normalised REE pattern showing LREE depletion and HREE enrichment (LREE/HREE= 0.01-0.67) (Fig. 10A). The REE pattern of zircons show negative Eu anomaly (0.01-0.90, average-0.43) and variably positive Ce anomaly (0.96-187.44, average-14.56). This HREE enriched REE pattern with negative Eu and positive Ce anomaly is typical for zircons occurring in granitoids (Fig. 10A) (Belousova et al., 2002). In addition, the Y concentrations of zircons varying from 411 to 18,223 ppm falls within the range of Y of zircons from granitoids (Belousova et al., 2002; Poller et al., 2001). The $(Lu)_N$ (where N= value normalised to chondrite) values varying from 344 to 14,955, are comparable to zircons from granitoids (500-20000 ppm; Hoskin and Ireland, 2000). A cross plot of Y (ppm) versus U (ppm) and Y (ppm) versus Yb/Sm has been used for discriminating the origin of zircon grains (Fig. 10B-C). The discrimination plots reflect that most of the samples fall in the field of granitoids (Fig. 10B-C). Thus, the trace element concentration obtained from the analyzed grains are typical for magmatic zircon.

4.4. Detrital zircon geochronology of the Cretaceous sedimentary rocks of the Jabalpur area, Central India

4.4.1. Jabalpur (White) Sandstone from the Jabalpur Formation

In total, 54 zircons were analyzed, of which 40 grains that provided concordant ages (<10% discordance) were considered for provenance and age interpretation. Most of the zircon grains are subhedral, subrounded, rarely rounded, while a few are subangular in shape, possibly implying short distance transport (Fig. 11). Zircons are variable in their size ranging in length from 60 to 215 μm (Fig. 11). The CL images reveal magmatic zoning in some grains whereas others show absence of zoning. Representative CL images of grains with their concordant ages are shown in Fig. 11. U-Pb Wetherill concordia plot and the age spectra obtained for these Late Jurassic-Early Cretaceous sandstones are presented in Fig. 12A, 12D. The probability density plot shows four age clusters between 2650-2450 Ma, 1800-1500 Ma, 1450-1300 Ma, and 1400-900 Ma for the Jabalpur Sandstone (Fig. 12A). The sample yielded major peaks at ~2488 Ma, 1665 Ma, 1084 Ma and a small peak at 1392 Ma. It is pertinent to note that this sample contains one grain of Neoproterozoic age (761±9 Ma) and a single youngest grain of 521±8 Ma. The zircons have Th/U ratios ranging from 0.14 to 1.87 with an average of 0.73 (Fig. 12G), indicating that the detrital zircons are predominantly of magmatic origin.

4.4.2. Green Sandstone and Upper Calcified Sandstone from the Lameta Formation

4.4.2.1. Green Sandstone

Eighty-one zircon grains were measured from the Green Sandstone sample, and 45 U-Pb ages were obtained after excluding the ages with higher discordance i.e., >10%. Most of the zircons range between 60 and 200 μm in size, and consist of elongated subhedral crystals, which are subangular to subrounded (Fig. 11). A few zircon grains show oscillatory zoning under SEM-CL images, while most of the detrital zircons have a faint internal structure (Fig. 11). U-Pb Concordia and Relative density probability plot of the sample shows age clusters between

2650-2450 Ma, 1850-1450 Ma, and 1400-1000 Ma (Fig 12B, E). The age spectra show prominent peaks at ~1118 Ma, 1514 Ma, 1699 Ma and 2580 Ma, along with the presence of detrital zircon grains showing ages of 752 Ma (n=2, 747±17 Ma, 755±14 Ma) and 548 Ma (n=2, 548±10 Ma, 548±9 Ma). U content in these zircons ranges in between 75 and 1775 ppm. Th/U ratio varies from 0.15 to 2.39 with an average of 1.05 and indicates magmatic origin for these zircon grains which is also consistent with their morphological characteristics.

4.4.2.2. Upper Calcified Sandstone

A total of 82 zircons were analyzed for their U-Pb ages, of which 58 concordant data points were obtained. The zircon grains from this sample are 50 to 200 μm in size and rounded to subhedral in shape (Fig. 11). Majority of the large sized grains are elongated whereas small grains are comparatively rounded in shape. SEM-CL analysis reveals that most zircons in the sample show oscillatory zoning (Fig. 11). The Upper Calcified Sandstone yields age spectra that are very similar to that of the Green Sandstone and Jabalpur Sandstone (Fig. 12C). Relative probability density plot shows the age population with clusters in the intervals of 2700-2400 Ma, 1900-1500 Ma, 1400-1200 Ma, and 1150-900 Ma. The sample shows four prominent peaks at ~2543 Ma, 1761 Ma, 1627 Ma, and 1066 Ma and a minor peak at 1379 Ma (Fig. 12C). The sample yields two zircon grains between 700-800 Ma i.e., 703±42 Ma and 796±16 Ma with one youngest grain of 541±11 Ma age. The U-Pb concordia plot shows multiple age clusters (Fig. 12F). The zircon grains have U content in the range of 86 to 1769 ppm, and Th/U ratio varies in between 0.07 to 2.40 with an average of 0.83, which is typical of magmatic zircons (Fig. 12I).

5. Discussion

5.1. Potential sources of detrital zircons of Upper Bhander Sandstone exposed in Bhopal and Bhimbetka

U-Pb detrital zircon geochronology of the Upper Bhander Sandstone at Bhopal and Bhimbetka shows an overall age range of 2600 to 1000 Ma with a single youngest grain of 770 ± 12Ma age. The documentation of zircon grains of 2450-2560 Ma age is comparable with the ~2480-2550 Ma age proposed for the emplacement of granitic suites in the Bundelkhand craton (Mondal et al., 2002; Verma et al., 2016; Kaur et al., 2016). The ages of the gneisses and granitoids of the Bundelkhand (3600-2400 Ma) basement rocks and the Aravalli BGC (3500-2500 Ma) indicate that the Archean and Paleoproterozoic zircons of the Vindhyan sandstones are largely derived from these terrains (Fig. 1A-B; Lan et al., 2020, 2021; Malone et al., 2008; Turner et al., 2014).

The detrital zircon cluster in the interval of 1500-1900 Ma and a small cluster between 2000-2100 Ma are more likely sourced from the Mahakoshal Supracrustal Belt (MSB) along the Satpura Mobile Belt in CITZ (Fig. 1B). The MSB lying in the vicinity of these Upper Bhander outcrops records magmatic rocks of 2300-1800 Ma age from its basal Chitrangi Formation (Khanna et al., 2017) and the overlying Parsoi Formation (1894.3 ± 9.4 Ma; Sharma et al., 2022). Furthermore, granites of ~1880 Ma, ~1780 Ma, ~1750 Ma (Bora et al., 2013; Bora and Kumar 2015), and ~1790 Ma (Yadav et al., 2020) ages have been reported from the MSB, suggesting an age bracket of 1880-1750 Ma for a tectonothermal event (Fig. 1B; Yadav et al., 2020) and this correlates well with the Upper Bhander zircon ages that clusters between 1900-1700 Ma. Madan Mahal granite (1695 ± 9Ma; Yadav et al., 2020) from the western part and Sidhi granite (1640 ± 9Ma; Yadav et a., 2020) from the eastern part of the MSB preserve records of post-collisional events (Fig 1B). The ages of these magmatic rocks are comparable with the age cluster between 1600-1700 Ma in the sample under discussion.

The samples show a significant distribution over a range of 1400-1600 Ma which is centered at ~1500 Ma. Igneous and metamorphic rocks of this range are also known from the CITZ as it records an orogenic event at ~1620-1540 Ma (Bhowmik et al., 2014; Chattopadhyay et al., 2020). The evidence of this orogenic event is preserved in the Sausar Mobile Belt (SMB) in the southern part of the CITZ, where felsic plutonism affected the SMB between 1620-1530 Ma (Fig. 1B; Ahmad et al., 2009; Bhowmik et al., 2011; Bhowmik, 2019; Chattopadhyay et al., 2020). The age of magmatism in the SMB is comparable with 1400-1600 Ma detrital zircon ages. Apart from this, the source for ~1600 Ma zircons could also be reworked sediments of the Porcellanite Formation and the Rampur Shale of Lower Vindhyans (Bickford et al., 2017; Mishra et al., 2018; Rasmussen et al., 2002; Ray, 2006). Granite magmatism at 1700-1800 Ma also affected the ADFB (Fig. 1B), making them a plausible source for these zircon grains.

A few grains of ~1000-1100 Ma age present in the samples are likely to be derived from the CITZ which experienced an ~1000 Ma orogeny (Fig. 1B). Geochronological data records 940-1060 Ma metamorphism in the SMB in response to collision of the North and South Indian tectonic blocks (Bhowmik et al., 2012). Early Neoproterozoic (1050-950 Ma) granite magmatism has also been reported from the Gavilgarh-Tan Shear Zone exposed in the CITZ (Fig. 1B; Chattopadhyay et al., 2020). Moreover, granitic intrusions of ~1000-1100 Ma reported from the Aravalli-BGC region and the Delhi Fold Belt can also be related with ~1000-1100 Ma zircon grains of this study (Just et al., 2011; Pandit et al., 2003; Turner et al., 2014).

A youngest single concordant grain has been recorded in the sandstone with the $^{206}Pb/^{238}U$ age of 770$\pm$12 Ma. No detrital zircon younger than ~900 Ma has been reported from the Upper Vindhyan sequence till date except one grain of 548 Ma from the Maihar sandstone (Lan et al., 2020). This age correlates with the Neoproterozoic magmatic events recorded from northwest India. The Abu-Sirohi corridor which lies between the Delhi Fold Belt and Malani Igneous Suite (MIS) terrane records granitic intrusions of Late Neoproterozoic (Fig. 1B and Table 1). This tectonically active region experienced magmatic activity and resultant emplacement of granites dated between 769-764 Ma (Fig. 1B; Ashwal et al., 2013). The rocks of the Eastern Ghat Mobile Belts (EGMB) also record Neoproterozoic tectono-metamorphic events (870-690

Ma; Chatterjee et al., 2017; Hippe et al., 2016) and Pan African thermal events (611-484 Ma; Upadhyay, 2008). However, the Satpura highlands (CITZ) that act as a barrier between the EGMB and the Vindhyan Basin, likely prevented the transport of the detritus from the EGMB (Turner et al., 2014). Rocks of ~770 Ma age have so far not been reported from north and central India. One possible source for the zircon of ~770 Ma age in the Upper Bhander sandstone could be the granites of ~700-800 Ma from NW India (Possibly MIS and its equivalent; Table 1).

The U-Pb detrital zircon geochronological data of the Upper Bhander Sandstone exposed in Bhopal and Bhimbetka (Bhopal Inlier) reflects a mixed source, which is also supported by petrographic observations and the whole rock geochemical study (Fig. 7A-F). A large variation in the Nd-isotopic values of siliciclastic rocks of the Bhander Group (Son Valley) reported by Chakrabarti et al. (2007) is also in agreement with the interpretation of a mixed provenance for these rocks. Co-Th-La-Sc systematics used to understand the source rocks for these sandstones suggest that the source for the Upper Bhander Sandstone (Bhopal inlier) includes both igneous and metamorphic rock suites from the CITZ and the Bundelkhand massif (Fig. 7F). The interpretation of modal data (Mohammadi et al., 2014; Banerjee and Banerjee, 2010), and the whole rock geochemical attributes (Banerjee and Banerjee, 2010) of the Upper Bhander Sandstone exposed in the vicinity of Bhopal indicates their derivation mainly from granitic plutons, and high/low grade metamorphic rocks, with a minor contribution from recycled sedimentary rocks (Banerjee and Banerjee, 2010; Mohammadi et al., 2014; Mohammadi et al., 2015). Furthermore, it is believed that the underlying Kaimur Group of Son Valley has largely received sediments from the Mahakoshal Belt (Mishra and Sen; 2012; Quasim et al., 2018). Combining past studies and the present geochronological data, potential sources for these zircons could be inferred as the Archean Bundelkhand Gneissic complex, gneissic and granitic rocks of the CITZ (mainly Mahakoshal Belt) which are exposed close to the Vindhyan Basin, and the recycled sedimentary rocks/sandstones of the Rewa and Kaimur Groups. It is important to note here that north, northwest and west directed paleocurrent patterns have been reported for the Upper Vindhyan sediments (Akhtar, 1978; Ansari, 1994; Bhattacharya and Morad, 1993; Verma and Shukla, 2015), which indicate that the detritus is largely coming from the south, southeast or east of the Vindhyan belt. Multiple lines of evidence including the north and northwest (west) directed paleocurrent patterns (Akhtar, 1978; Ansari, 1994; Bhattacharya and Morad, 1993; Raza and Casshyap, 1996; Verma and Shukla, 2015) and detrital zircon geochronology suggest the Satpura-Mahakoshal/Bijawar highlands (CITZ) lying in the south and southeast (east) of the basin as the dominant source of detritus for the Upper Vindhyan sandstones exposed in and around Bhopal (Fig. 13; Chakraborty, 2006). However, rocks from the ADFB may also constitute a secondary (distal) source for these sediments.

5.2. Potential sources of detrital zircons of the Cretaceous sandstones of Jabalpur

The synthesis of detrital zircon geochronology reveals that the age spectra of zircons from the Cretaceous sandstones of Jabalpur area i.e., Jabalpur Sandstone, Green Sandstone and the Upper Calcified Sandstone show a similar pattern (Fig. 12 A-C). This similarity suggests that common sources have contributed sediments to these rocks and/or reworking of underlying sedimentary rocks produced similar ages. The geochronology of these rocks clearly indicates that the detritus predominantly contains a record of Paleoproterozoic and Mesoproterozoic zircons exhibiting a major cluster between 1500-1800 Ma with peaks at either ~1600 Ma or ~1700 Ma (Fig. 13). These peaks correlate with the age of the Madan Mahal granites (1695 ± 9 Ma; Yadav et al., 2020) that are well exposed in the Jabalpur region and located in the western part of the MSB. The zircon ages clustered between 900 and 1100 Ma with a peak at 1000 Ma, are correlated with the rocks of the CITZ (Fig. 1B, 13). It has been observed that detrital zircon grains of 1500-1800 Ma and 900-1100 Ma age brackets are also present in the rocks of the Vindhyan Supergroup (Fig 2B, 13). Despite the absence of rocks of 500-750 Ma age range in

Central India, especially in the Narmada-Son Valley, the Cretaceous sandstones exhibit a few detrital zircons of ~520-550 Ma and ~700-800 Ma age. The geochronological results of this study indicate that these Cretaceous sediments contain a variety of age populations and this spread of age could be due to multiple sources. The discrimination diagram, ICV value, and trace element ratios (Fig. 7B-F) altogether point to a mixed source for these sediments ranging from the granitic, metasedimentary rocks of MSB to the recycled sediments from the Vindhyans.

Sediments belonging to the Jabalpur Formation were deposited by rivers flowing from the north and northwest directions (Chanda and Bhattacharya, 1966; Tandon, 2002) (Fig. 4C, E). In addition, Casshyap and Khan (2000) suggested that prior to the deposition of the Bagra Formation underlying the Jabalpur Formation, the tectonic disturbance along the Narmada-Son Lineament caused an upliftment of the Mahakoshal/Bijawar and Vindhyan cratonic blocks in Central India. Similar to the Early Cretaceous Jabalpur Formation, southerly to southwesterly flowing ephemeral streams deposited the Green Sandstone of Lameta Formation (Fig. 4C, E; Chanda and Bhattacharya, 1966; Tandon, 2002). The paleoflow patterns of the Jabalpur sandstone and the Green Sandstone indicate that the potential source rocks are likely distributed to the northern or the northeastern side of these outcrops. The paleoslope and paleoflow direction of channels, geochemical attributes (Co/Th and La/Sc ratio; Fig. 7B-F), and the predominance of 1500-1800 Ma zircon age cluster, combined together suggest the Mahakoshal Belt to be the major source terrains for these Cretaceous sandstones (Fig. 4C).

Considering the paleoslope (Casshyap and Khan, 2000) and present distribution of rocks of the Vindhyan Supergroup in and around the Jabalpur area, especially to the north and northeast of these Cretaceous sedimentary strata (Fig. 4C), it is likely that recycled detritus was supplied from the Vindhyan Supergroup. The recycled nature is also interpreted through the whole rock geochemistry of the Cretaceous sandstones (Fig. 7B-F). In order to ascertain that the Vindhyan

Supergroup is one of the potential sources for these sandstones, the age spectra of the Vindhyan sandstones have been compared with that of the Cretaceous sandstone samples (Fig. 13). The detrital zircon spectra of the Vindhyan samples from the Son Valley are broadly similar to those of the age clusters present in the Cretaceous sandstones (Fig. 13). The zircon U-Pb age distributions of the Cretaceous sandstones show that a higher proportion of detrital zircons with age groups of 1500-1900 Ma, 900-1300 Ma and 2400-3000 Ma correlate well with the zircon age peaks present in the Vindhyan samples (Fig. 13). Furthermore, the zircon grains of ~550 Ma and ~770 Ma recorded in these stratigraphically younger sandstones are similarly present Upper Bhander sandstone (Bhopal and Maihar) (Fig. 13). The similarity in the age distribution and the geochemical composition also indicates that both the groups have possibly received detritus from similar source terrains. As noted earlier, the analysis of stratigraphic data reveals the absence of Late Neoproterozoic-Cambrian rocks in central India. Rocks of this age range corresponding to the Malani Igneous events and Pan-African orogeny are distributed in the Northwestern (e.g., Ashwal et al, 2013; Rathore et al., 1999; Sen et al., 2013; Wang et al., 2017, 2018), northern (e.g., Dhiman and Singh, 2021; Islam et al., 1999; Majumdar and Dutta, 2016; Miller et al., 2001; Singh, 2020) and southern (e.g., Braun, 2006; Rajesh, 1996; Santosh et al., 2003) parts of India (Fig. 14). The south-southwest directed local and ephemeral fluvial channels (Fig. 4C, 5) that deposited the Cretaceous sediments (Casshyap and Khan, 2000; Chanda and Bhattacharya, 1966; Tandon, 2002) indicate that it is unlikely for the detritus to have been derived from these terrains.

Underlying Gondwana sediments could also provide younger zircons between 500-750 Ma. The reported U-Pb zircon ages of the Gondwana sandstones show strong clustering between 500-1000 Ma ages with abundant 500-750 Ma zircon grains (Veevers and Saeed, 2009). In contrast, the Cretaceous sediments of Jabalpur show only a few zircon grains of this age range (2 grains from each sandstone). Late Jurassic and Early Cretaceous uplift of the Mahakoshal and Vindhyan terrane in the Satpura basin, reversal of paleoslope (north to south; Casshyap and Khan, 2000), geochemical signature (Fig. 7A-F) and comparable detrital zircon age distributions of the Upper Vindhyan and Cretaceous sandstones altogether suggest that the young zircons in the Cretaceous sandstones of Jabalpur are most likely derived from the Vindhyan sandstones. Another possibility is that the Late Neoproterozoic-Early Cambrian rocks might have been exposed in the past in Central India, which have been later removed by erosion or have remained buried underneath the Deccan traps.

5.3. Post-1000 Ma zircon grains: their bearing on the depositional age of Upper Vindhyan succession

It is noteworthy that earlier paleontological findings (Table 3) have been used to assign an Ediacaran age (<1000 Ma) for the Bhander Group in the Son Valley Sector. The Upper Bhander Sandstone from Maihar and Bhopal region contains post-1000 Ma zircon grains of ~548 Ma and ~770 Ma age respectively. Moreover, the detrital zircon ages from the Cretaceous sandstone in Jabalpur reveal supply of detritus from a source that contains younger zircons (~500-550 Ma and ~770 Ma). The zircon grains younger than ~1000 Ma in the Cretaceous sediments are likely recycled from the Vindhyans as can be inferred from the paleoslope and paleoflow direction.

The detrital zircon geochronology of the Upper Bhander Sandstone in the Rajasthan Sector also suggests ~1000 Ma closure age for the sedimentation of Upper Vindhyan (Fig. 15B; Malone et al., 2008). In contrast, a Cryogenian (850-630 Ma) age marker microfossil *Trachyhystrichosphaera* from the Sirbu Shale Formation of Bhander Group, Rajasthan (Srivastava, 2009) and ~770 Ma age (on the basis of Sr isotope stratigraphy coupled with Pb-Pb age) of Balwan Limestone (George et al., 2018, Gopalan et al., 2013), overlying the Upper Bhander Sandstone suggest post 1000 Ma sedimentation in the Rajasthan sector of the

Vindhyan Basin (Fig. 15B). The Proterozoic sedimentary packages of the Lesser Himalayan sector and the Ganga Valley have been linked with the rocks of the Vindhyan Basin in the cratonic area (McKenzie et al., 2011; Xiao et al., 2016). The siliciclastic rocks of the Blaini Formation (Cryogenian) and Krol and Infra Krol (Ediacaran) successions of the Outer Lesser Himalaya have the Neoproterozoic zircon populations (Fig. 15D; McKenzie et al., 2011; Hofmann et al., 2011). Considering the two young zircon ages i.e., 548 Ma and 770 Ma (<1000 Ma) reported from the Upper Bhander Sandstone as robust data points, a ~1000 Ma age for the termination of Upper Vindhyan sedimentation needs re-examination.

6. Conclusion

1. Magmatic and metasedimentary rocks exposed in the Satpura Mobile Belt (CITZ), south and east of the Vindhyan Basin, are considered as the major sources of the detritus for the Upper Bhander Sandstone exposed in the Bhopal inlier. However, the underlying older Vindhyan sedimentary rocks and those from the Bundelkhand craton and Aravalli-Delhi Fold Belt likely also acted as provenance for the Upper Vindhyan sandstone.
2. The occurrence of zircon grains of ~548 Ma (Maihar) and ~770 Ma (Bhimbetka) taken together with the previously published paleobiological evidences serve as a pointer that the Vindhyan sedimentation could have extended into the Tonian and possibly into the Ediacaran (?).
3. Cretaceous sandstones of the Upper Gondwana and Lameta successions show similar peaks as those of the sandstones of the Vindhyan Supergroup including the presence of younger grains of ~500-550 Ma and ~700-800 Ma age. Some of these ages may correspond to the final stages of closure and inversion of the Vindhyan basin and the related generation of recycled detritus from the basin’s marginal areas.

Acknowledgements

The authors would like to thank The Indian Institute of Science Education and Research Bhopal for all resources including doctoral student fellowship to VK. We thank Prof. Gregory John Retallack for careful reading of an earlier version of this manuscript that resulted in its improvement. We thank Superintending Archaeologist, Archaeological Survey of India (ASI), Bhopal for their approval to take samples from Bhimbetka. This research is partially supported by an MHRD (FAST 2016/17) grant.

References

Ahmad, T., Kaulina, T. V., Wanjari, N., Mishra, M. K., Nitkina, E. A., 2009. U–Pb zircon chronology and Sm–Nd isotopic characteristics of the Amgaon and Tirodi Gneissic Complex, Central Indian Shield: constraints on Precambrian crustal evolution. In Precambrian continental growth and tectonism. Excel India Publishers New Delhi 137-138.

Akhtar, K., 1978. Paleogeography and sediment dispersal patterns of the Proterozoic Bhander Group, western India. Palaeogeography, Palaeoclimatology, Palaeoecology 24, 327-357.

Ansari, A.A., 1994. Facies Analysis, petrographic composition and nature of provenance of Bhander Sandstone around Bhopal, M.P. PhD thesis. Aligarh Muslim University.

Ashwal, L. D., Solanki, A. M., Pandit, M. K., Corfu, F., Hendriks, B. W. H., Burke, K., Torsvik, T. H., 2013. Geochronology and geochemistry of Neoproterozoic Mt. Abu granitoids, NW India: Regional correlation and implications for Rodinia paleogeography. Precambrian Research 236, 265-281.

Azmi, R. J., 1998. Fossil discoveries in India. Science 282, 627-628.

Azmi, R. J., Joshi, D., Tiwari, B. N., Joshi, M. N., Srivastava, S. S., 2008. A synoptic view on the current discordant geo-and biochronological ages of the Vindhyan Supergroup, central

India. Journal of Himalayan Geology 29, 177-191.

Banerjee, A., Banerjee, D. M., 2010. Modal analysis and geochemistry of two sandstones of the Bhander Group (Late Neoproterozoic) in parts of the Central Indian Vindhyan basin and their bearing on the provenance and tectonics. Journal of earth system science 119, 825.

Banerjee, A., Sequeira, N., Bhattacharya, A., 2021. Tectonics of the Greater India Proterozoic Fold Belt, with emphasis on the nature of curvature of the belt in west-central India. Earth-Science Reviews, 103758.

Basu, A., Bickford, M. E., 2015. An alternate perspective on the opening and closing of the intracratonic Purana basins in peninsular India. Journal of the Geological Society of India 85, 5-25.

Basu, P., Banerjee, A., Chakrabarti, R., 2021. A combined geochemical, Nd, and stable Ca isotopic investigation of provenance, paleo-depositional setting and sub-basin connectivity of the Proterozoic Vindhyan Basin, India. Lithos 388, 106059.

Belousova, E. A., Griffin, W. L., O'Reilly, S. Y., Fisher, N. L., 2002. Igneous zircon: trace element composition as an indicator of source rock type. Contributions to mineralogy and petrology 143, 602-622.

Bengtson, S., Belivanova, V., Rasmussen, B., Whitehouse, M., 2009. The controversial "Cambrian" fossils of the Vindhyan are real but more than a billion years older. Proceedings of the National Academy of Sciences, 106, 7729-7734.

Bengtson, S., Sallstedt, T., Belivanova, V., Whitehouse, M. (2017). Three-dimensional preservation of cellular and subcellular structures suggests 1.6 billion-year-old crown-group red algae. PLoS Biology 15(3), e2000735.

Bhattacharyya, A., Morad, S., 1993. Proterozoic braided ephemeral fluvial deposits: an example from the Dhandraul Sandstone Formation of the Kaimur Group, Son Valley, central India. Sedimentary Geology, 84, 101-114.

Bhowmik, S. K., Wilde, S. A., Bhandari, A., Basu Sarbadhikari, A., 2014. Zoned monazite and zircon as monitors for the thermal history of granulite terranes: an example from the Central Indian Tectonic Zone. Journal of Petrology 55, 585-621.

Bhowmik, S. K., Wilde, S. A., Bhandari, A., Pal, T., Pant, N. C., 2012. Growth of the Greater Indian Landmass and its assembly in Rodinia: geochronological evidence from the Central Indian Tectonic Zone. Gondwana Research 22, 54-72.

Bhowmik, S. K., 2019. The current status of orogenesis in the Central Indian Tectonic Zone: A view from its Southern Margin. Geological Journal 54, 2912-2934.

Bhowmik, S. K., Wilde, S. A., Bhandari, A., 2011. Zircon U-Pb/Lu-Hf and monazite chemical dating of the Tirodi biotite gneiss: implication for latest Palaeoproterozoic to Early Mesoproterozoic orogenesis in the Central Indian Tectonic Zone. Geological Journal 46, 574-596.

Bickford, M. E., Mishra, M., Mueller, P. A., Kamenov, G. D., Schieber, J., Basu, A., 2017. U-Pb age and Hf isotopic compositions of magmatic zircons from a rhyolite flow in the Porcellanite Formation in the Vindhyan Supergroup, Son Valley (India): implications for its tectonic significance. The Journal of Geology 125, 367-379.

Bickford, M. E., Basu, A., 2021. “Towards resolving the ‘jigsaw puzzle’and age-fossil inconsistency within East Gondwana”: A comment. Precambrian Research 352, 105881.

Biju-Sekhar, S., Yokoyama, K., Pandit, M. K., Okudaira, T., Yoshida, M., Santosh, M., 2003. Late Paleoproterozoic magmatism in Delhi Fold Belt, NW India and its implication: evidence from EPMA chemical ages of zircons. Journal of Asian Earth Sciences, 22, 189-207.

Bora, S., Kumar, S., Yi, K., Kim, N., Lee, T. H., 2013. Geochemistry and U–Pb SHRIMP zircon chronology of granitoids and microgranular enclaves from Jhirgadandi pluton of Mahakoshal Belt, Central India Tectonic Zone, India. Journal of Asian Earth Sciences 70, 99-114.

Bora, S., Kumar, S., 2015. Geochemistry of biotites and host granitoid plutons from the Proterozoic Mahakoshal Belt, central India tectonic zone: implication for nature and tectonic setting of magmatism. International Geology Review 57, 1686-1706.

Bose, P. K., Sarkar, S., Chakrabarty, S., and Banerjee, S., 2001. Overview of the Meso-to Neoproterozoic evolution of the Vindhyan basin, central India. Sedimentary Geology 141, 395-419.

Braun, I., 2006. Pan-African granitic magmatism in the Kerala Khondalite Belt, southern India. Journal of Asian Earth Sciences 28, 38-45.

Casshyap, S. M., Khan, A., 2000. Tectono-sedimentary evolution of the Gondwanan Satpura Basin of central India: evidence of pre-Trap doming, rifting and paleoslope reversal. Journal of African Earth Sciences 31, 65-76.

Chakrabarti, R., Basu, A. R., Chakrabarti, A., 2007. Trace element and Nd-isotopic evidence for sediment sources in the mid-Proterozoic Vindhyan Basin, central India. Precambrian Research 159, 260-274.

Chakraborty, C., 2006. Proterozoic intracontinental basin: the Vindhyan example. Journal of Earth System Science 115, 3-22.

Chakraborty, P. P., Tandon, S. K., Roy, S. B., Saha, S., Paul, P. P., 2020. Proterozoic sedimentary basins of India. In Geodynamics of the Indian Plate. Springer, Cham 145-177.

Chanda, S. K., Bhattacharyya, A., 1966. A re-evaluation of the stratigraphy of the Lameta-Jabalpur contact around Jabalpur, MP. Journal of Geological Society of India 7, 92-99.

Chatterjee, A., Das, K., Bose, S., Ganguly, P., Hidaka, H., 2017. Zircon U–Pb SHRIMP and monazite EPMA U–Th–total Pb geochronology of granulites of the western boundary, Eastern Ghats Belt, India: a new possibility for Neoproterozoic exhumation history. Geological Society, London, Special Publications 457, 105-140.

Chattopadhyay, A., Bhowmik, S. K., Roy, A., 2020. Tectonothermal evolution of the Central Indian Tectonic Zone and its implications for Proterozoic supercontinent assembly: the current status. Episodes, 43, 132-144.

Chattopadhyay, A., Das, K., Hayasaka, Y., Sarkar, A., 2015. Syn-and post-tectonic granite plutonism in the Sausar Fold Belt, central India: age constraints and tectonic implications. Journal of Asian Earth Sciences 107, 110-121.

Colleps, C. L., McKenzie, N. R., Sharma, M., Liu, H., Gibson, T. M., Chen, W., Stockli, D. F., 2021. Zircon and apatite U-Pb age constraints from the Bundelkhand craton and Proterozoic strata of central India: Insights into craton stabilization and subsequent basin evolution. Precambrian Research 362, 106286.

Collins, A. S., Pisarevsky, S. A., 2005. Amalgamating eastern Gondwana: the evolution of the Circum-Indian Orogens. Earth-Science Reviews 71, 229-270.

Cox, R., Lowe, D. R., Cullers, R. L., 1995. The influence of sediment recycling and basement composition on evolution of mudrock chemistry in the southwestern United States. Geochimica et Cosmochimica Acta 59(14), 2919-2940.

Deb, M., Thorpe, R. I., Krstic, D., Corfu, F., Davis, D. W., 2001. Zircon U–Pb and galena Pb isotope evidence for an approximate 1.0 Ga terrane constituting the western margin of the Aravalli–Delhi orogenic belt, northwestern India. Precambrian Research 108, 195-213.

De, C., 2003. Possible organisms similar to Ediacaran forms from the Bhander Group, Vindhyan Supergroup, late Neoproterozoic of India. Journal of Asian Earth Sciences 21, 387-395.

De, C., 2006. Ediacara fossil assemblage in the upper Vindhyans of Central India and its significance. Journal of Asian Earth Sciences 27, 660-683.

Dey, B., Das, K., Dasgupta, N., Bose, S., Hidaka, H., Ghatak, H., 2019. Zircon U–Pb (SHRIMP) ages of the jahazpur granite and mangalwar gneiss from the Deoli-Jahazpur sector, Rajasthan, NW India: a preliminary reappraisal of stratigraphic correlation and implications to crustal growth. In Geological Evolution of the Precambrian Indian Shield. Springer, Cham 39-56.

Dev, J. A., Tomson, J. K., Sorcar, N., Nandakumar, V., 2021. Combined U-Pb/Hf isotopic studies and phase equilibrium modelling of HT-UHT metapelites from Kambam Ultrahigh temperature Belt, South India: Constraints on tectonothermal history of the terrain. Lithos 106531.

De Wall, H., Pandit, M. K., Donhauser, I., Schöbel, S., Wang, W., Sharma, K. K., 2018. Evolution and tectonic setting of the Malani–Nagarparkar igneous suite: A neoproterozoic silicic-dominated large igneous province in NW India-SE Pakistan. Journal of Asian Earth Sciences 160, 136-158.

Dhiman, R., Singh, S., 2021. Neoproterozoic and Cambro-Ordovician magmatism: episodic growth and reworking of continental crust, Himachal Himalaya, India. International Geology Review 63, 422-436.

Dogra, N. N., Singh, R. Y., Kulshreshtha, S. K., 1994. Palynostratigraphy of infra-trappean Jabalpur and Lameta formations (Lower and Upper Cretaceous) in Madhya Pradesh, India. Cretaceous research 15, 205-215.

Dogra, N. N., Singh, R. Y., Kumar, S., 2010. The Lithostratigraphic Status of Jabalpur and Lameta Formations and their Palynological Constraints on the Age and Environment. Gondwana Geological Magazine 25, 185-194.

D'Souza, J., Prabhakar, N., Xu, Y., Sharma, K. K., Sheth, H., 2019. Mesoarchaean to Neoproterozoic (3.2–0.8 Ga) crustal growth and reworking in the Aravalli Craton, northwestern India: Insights from the Pur-Banera supracrustal belt. Precambrian Research 332, 105383.

Geological Survey of India. 1998. Bhopal Quadrangle Geological Map of 56E, Madhya Pradesh, Geological Survey of India Publication.

George, B. G., Ray, J. S., 2017. Provenance of sediments in the Marwar Supergroup, Rajasthan, India: Implications for basin evolution and Neoproterozoic global events. Journal of Asian Earth Sciences 147, 254-270.

George, B. G., Ray, J. S., Shukla, A. D., Chatterjee, A., Awasthi, N., Laskar, A. H., 2018. Stratigraphy and geochemistry of the Balwan Limestone, Vindhyan Supergroup, India: evidence for the Bitter Springs $\delta^{13}C$ anomaly. Precambrian Research 313, 18-30.

George, B. G., 2021. On Chhoti Khatu volcanics of Rajasthan and its relationship with the Malani magmatism: A geochemical study. Journal of Earth System Science 130(2), 1-9.

Gilleaudeau, G. J., Sahoo, S. K., Kah, L. C., Henderson, M. A., Kaufman, A. J., 2018. Proterozoic carbonates of the Vindhyan Basin, India: Chemostratigraphy and diagenesis. Gondwana Research 57, 10-25.

Gopalan, K., Kumar, A., Kumar, S., Vijayagopal, B., 2013. Depositional history of the Upper Vindhyan succession, central India: time constraints from Pb–Pb isochron ages of its carbonate components. Precambrian Research 233, 108-117.

Gregory, L.C., Meert, J.G., Pradhan, V., Pandit, M.K., Tamrat, E., and Malone, S.J., 2006. A paleomagnetic and geochronologic study of the Majhgawan kimberlite, India: Implications for the age of the Upper Vindhyan Supergroup: Precambrian Research 149, 65–75.

Hippe, K., Möller, A., von Quadt, A., Peytcheva, I., Hammerschmidt, K., 2016. Zircon geochronology of the Koraput alkaline complex: insights from combined geochemical and U–Pb–Hf isotope analyses, and implications for the timing of alkaline magmatism in the

Eastern Ghats Belt, India. Gondwana Research 34, 205-220.

Hofmann, M., Linnemann, U., Rai, V., Becker, S., Gärtner, A., Sagawe, A., 2011. The India and South China cratons at the margin of Rodinia—Synchronous Neoproterozoic magmatism revealed by LA-ICP-MS zircon analyses. Lithos 123, 176-187.

Hoskin, P. W., Ireland, T. R., 2000. Rare earth element chemistry of zircon and its use as a provenance indicator. Geology 28, 627-630.

Islam, R., Upadhyay, R., Ahmad, T., Thakur, V. C., Sinha, A. K., 1999. Pan-African magmatism, and sedimentation in the NW Himalaya. Gondwana Research 2, 263-270.

Just, J., Schulz, B., de Wall, H., Jourdan, F., Pandit, M. K., 2011. Monazite CHIME/EPMA dating of Erinpura granitoid deformation: Implications for Neoproterozoic tectono-thermal evolution of NW India. Gondwana Research 19, 402-412.

Kale, V. S., 2016. Proterozoic basins of Peninsular India: status within the global Proterozoic systems. Proceedings of the Indian National Science Academy 82, 461-477.

Kaur, P., Zeh, A., Chaudhri, N., Eliyas, N., 2016. Unravelling the record of Archaean crustal evolution of the Bundelkhand Craton, northern India using U–Pb zircon–monazite ages, Lu–Hf isotope systematics, and whole-rock geochemistry of granitoids. Precambrian Research 281, 384-413.

Kaur, P., Chaudhri, N., Raczek, I., Kroener, A., Hofmann, A. W., 2007. Geochemistry, zircon ages and whole-rock Nd isotopic systematics for Palaeoproterozoic A-type granitoids in the northern part of the Delhi belt, Rajasthan, NW India: implications for late Palaeoproterozoic crustal evolution of the Aravalli craton. Geological Magazine 144, 361-378.

Kaur, P., Chaudhri, N., Raczek, I., Kröner, A., Hofmann, A. W., 2009. Record of 1.82 Ga Andean-type continental arc magmatism in NE Rajasthan, India: insights from zircon and Sm–Nd ages, combined with Nd–Sr isotope geochemistry. Gondwana Research 16, 56-

71.

Kaur, P., Chaudhri, N., Raczek, I., Kröner, A., Hofmann, A. W., Okrusch, M., 2011. Zircon ages of late Palaeoproterozoic (ca. 1.72–1.70 Ga) extension-related granitoids in NE Rajasthan, India: regional and tectonic significance. Gondwana Research 19, 1040-1053.

Kaur, P., Zeh, A., Chaudhri, N., 2014. Characterisation and U–Pb–Hf isotope record of the 3.55 Ga felsic crust from the Bundelkhand Craton, northern India. Precambrian Research 255, 236-244.

Kaur, P., Zeh, A., Chaudhri, N., Dutta, P., 2014. Detrital zircon U-Pb-Hf isotope record of conglomerates in the southern Aravalli orogen, NW India: Implications for stratigraphy, provenance and Archean to Paleoproterozoic crustal evolution. Precanbrian Research 379, Article 106800.

Khanna, T. C., Rao, D. S., Bizimis, M., Satyanarayanan, M., Krishna, A. K., Sai, V. S., 2017. ~ 2.1 Ga intraoceanic magmatism in the Central India Tectonic Zone: Constraints from the petrogenesis of ferropicrites in the Mahakoshal supracrustal belt. Precambrian Research 302, 1-17.

Kumar, A., Gopalan, K., Rajagopalan, G., 2001. Age of the Lower Vindhyan sediments, central India. Current Science-Bangalore-, 81, 806-808.

Kumar, B., Sharma, S. D., Sreenivas, B., Dayal, A. M., Rao, M. N., Dubey, N., Chawla, B. R., 2002. Carbon, oxygen and strontium isotope geochemistry of Proterozoic carbonate rocks of the Vindhyan Basin, central India. Precambrian Research 113, 43-63.

Kumar S. 2012. Stratigraphy and correlation of the Neoproterozoic deposits of central and western India: An overview. Geological Society Special Publication 366, 75-90.

Kumar, S., Ahmad, S., 2016. Problematic structures from the Ediacaran Jodhpur Sandstone, Rajasthan, India, and their possible affinity. Journal of the Palaeontological Society of India 61, 63-73.

Kumar, S., Pandey, S. K., 2008. Arumberia and associated fossils from the Neoproterozoic Maihar Sandstone, Vindhyan Supergroup, Central India. Journal of the Palaeontological Society of India 53, 83-97.

Kumar, S., Pandey, S. K., 2010. Trace fossils from the Nagaur Sandstone, Marwar Supergroup, Dulmera area, Bikaner district, Rajasthan, India. Journal of Asian Earth Sciences 38, 77-85.

Kumar, S., Sharma, M., 2012. Vindhyan Basin, Son Valley Area Central India. Palaeontological Society of India.

Kumar, S., Srivastava, P., 2003. Carbonaceous megafossils from the Neoproterozoic Bhander Group, Central India. Journal of the Palaeontological Society of India, 48, 139-154.Lan, Z., Pandey, S. K., Zhang, S., Sharma, M., Gao, Y., Wu, S., 2021. Precambrian crustal evolution in Northern Indian Block: Evidence from detrital zircon U-Pb ages and Hf-isotopes. Precambrian Research 361, 106238.

Lan, Z., Zhang, S., Li, X. H., Pandey, S. K., Sharma, M., Shukla, Y., Zhai, M., 2020. Towards resolving the ‘jigsaw puzzle’and age-fossil inconsistency within East Gondwana. Precambrian Research 345, 105775.

Ludwig, K. R., 2012. Isoplot 4.15: a geochronological toolkit for Microsoft Excel. Berkeley Geochronology Center Special Publication, 5.

Maithy, P. K., Kumar, G., Prasad, B., 2007. Obruchevella and other terminal Proterozoic (Vendian) organic walled microfossils from the Bhander Group (Vindhyan Supergroup), Madhya Pradesh. Journal of Geological Society of India 70, 373-375.

Malone, S. J., Meert, J. G., Banerjee, D. M., Pandit, M. K., Tamrat, E., Kamenov, G. D., Sohl, L. E., 2008. Paleomagnetism and detrital zircon geochronology of the Upper Vindhyan Sequence, Son Valley and Rajasthan, India: A ca. 1000 Ma closure age for the Purana Basins?. Precambrian Research 164, 137-159.

Majumdar, D., Dutta, P., 2016. Geodynamic evolution of a Pan-African granitoid of extended Dizo Valley in Karbi Hills, NE India: evidence from geochemistry and isotope geology. Journal of Asian Earth Sciences 117, 256-268.

McKenzie, N. R., Hughes, N. C., Myrow, P. M., Xiao, S., Sharma, M., 2011. Correlation of Precambrian–Cambrian sedimentary successions across northern India and the utility of isotopic signatures of Himalayan lithotectonic zones. Earth and Planetary Science Letters 312, 471-483.

McLennan, S. M., Hemming, S., Mcdaniel, D., Hanson, G., 1993. Geochemical approaches to sedimentation, provenance, and tectonic. Geological Society of America Special Papers 284, 21‑40.

Meert, J. G., Pandit, M. K., 2015. Precambrian evolution of Peninsular India and its link to basin evolution. Precambrian Basins of India: Stratigraphic and Tectonic Criteria (Eds: Mazumder. R, and Eriksson, PG). Geol. Soc. Lon. Memoirs 43, 29-54.

Meert, J. G., Pandit, M. K., Pradhan, V. R., Banks, J., Sirianni, R., Stroud, M., Newstead, B., Gifford, J. (2010). Precambrian crustal evolution of Peninsular India: a 3.0 billion year odyssey. Journal of Asian Earth Sciences 39(6), 483-515.

Meert, J. G., Pandit, M. K., Venkateshwarlu, M., Rao, J. M., 2013. Paleomagnetism of Bhander Sediments from Bhopal Inlier, Vindhyan Supergroup. Journal of the Geological Society of India 82, 588.

Meert, J.G., Pandit, M.K., Kwafo, S. and Singha, A., 2023. Stinging News:'Dickinsonia'discovered in the Upper Vindhyan of India Not Worth the Buzz. Gondwana Research.

Miller, C., Thöni, M., Frank, W., Grasemann, B., Klötzli, U., Guntli, P., Draganits, E., 2001. The early Palaeozoic magmatic event in the Northwest Himalaya, India: source, tectonic setting and age of emplacement. Geological Magazine 138, 237-251.

Mishra, M., Bickford, M. E., Basu, A., 2018. U-Pb age and chemical composition of an ash bed in the Chopan Porcellanite Formation, Vindhyan Supergroup, India. The Journal of Geology 126, 553-560.

Mishra, M., Sen, S., 2012. Provenance, tectonic setting and source-area weathering of Mesoproterozoic Kaimur Group, Vindhyan Supergroup, Central India. Geologica Acta, 283-293.

Mohammadi, N., Rais, S., Habib, T., 2014. Provenance, tectonic setting and paleoclimate of Upper Bhander Sandstone in parts of Raisen district of Madhya Pradesh (India). International Journal of Advance Earth and Environment Science 2, 39-45.

Mohammadi, N., 2015. Sedimentological and remote Sensing Studies on Vindhyan Ssupergroup, Raisen District, Madhya Pradesh. PhD thesis. Aligarh Muslim University (121).

Mondal, M. E. A., Goswami, J. N., Deomurari, M. P., Sharma, K. K., 2002. Ion microprobe 207Pb/206Pb ages of zircons from the Bundelkhand massif, northern India: implications for crustal evolution of the Bundelkhand–Aravalli protocontinent. Precambrian Research 117, 85-100.

Nesbitt, H. W., Young, G. M., 1982. Early Proterozoic climates and plate motions inferred from major element chemistry of lutites. Nature 299, 715‑717.

Pandey, S.K., Ahmad, S. and Sharma, M., 2023. For Preprint.

Pandey, S. K., Sharama, M., 2017. Enigmatic Ediacaran Megascopic bedding plane structures on the Sonia Sandstone, the Jodhpur Group, Marwar Supergroup, India; Seaweed or problematica? Geological Journal 52, 784-807..

Pandit, M. K., Carter, L. M., Ashwal, L. D., Tucker, R. D., Torsvik, T. H., Jamtveit, B., Bhushan, S. K., 2003. Age, petrogenesis and significance of 1 Ga granitoids and related rocks from the Sendra area, Aravalli Craton, NW India. Journal of Asian Earth

Sciences 22, 363-381.

Pandit, M. K., Kumar, H., Wang, W., 2021. Geochemistry and geochronology of A-type basement granitoids in the north-central Aravalli Craton: Implications on Paleoproterozoic geodynamics of NW Indian Block. Geoscience Frontiers 12, 101084.

Pati, J.K., 1997. Specialized thematic studies of Bundelkhand Granitoids for appraisal of the mode of occurrence of molybdenum and associated mineralization, Rauli Kalyanpur area, Banda districts, U.P. Geological Survey of India Records 129, 144-146.

Paton, C., Hellstrom, J., Paul, B., Woodhead, J., Hergt, J., 2011. Iolite: Freeware for the visualisation and processing of mass spectrometric data. Journal of Analytical Atomic Spectrometry, 26, 2508-2518.

Pearce, N. J., Perkins, W. T., Westgate, J. A., Gorton, M. P., Jackson, S. E., Neal, C. R., Chenery, S. P., 1997. A compilation of new and published major and trace element data for NIST SRM 610 and NIST SRM 612 glass reference materials. Geostandards newsletter 21, 115-144.

Petrus, J. A., Kamber, B. S., 2012. VizualAge: A novel approach to laser ablation ICP-MS U-Pb geochronology data reduction. Geostandards and Geoanalytical Research 36, 247-270.

Poller, U., Huth, J., Hoppe, P., Williams, I. S., 2001. REE, U, Th, and Hf distribution in zircon from western Carpathian Variscan granitoids: a combined cathodoluminescence and ion microprobe study. American Journal of Science 301, 858-867.

Prasad, B., Uniyal, S. N., Asher, R., 2005. Organic-walled microfossils from the Proterozoic Vindhyan Supergroup of Son Valley, Madhya Pradesh, India.

Quasim, M. A., Hota, R. N., Ahmad, A. H. M., Albaroot, M., 2018. An approach to provenance and tectonic setting of the Proterozoic Upper Kaimur Group sandstones, Son Valley: constraints from framework mineralogy and heavy mineral analysis. Himalayan Geology, 39, 145-160.

Rajesh, H. M., Santosh, M., Yoshida, M., 1996. The felsic magmatic province in East Gondwana: implications for Pan-African tectonics. Journal of Southeast Asian Earth Sciences 14, 275-291.

Ramakrishnan, M., Vaidyanadhan, R., 2010. Geology of India (vol. 1 & 2). GSI Publications, 2(1).

Rathore, S. S., Venkatesan, T. R., Srivastava, R. K., 1999. Rb-Sr isotope dating of Neoproterozoic (Malani Group) magmatism from Southwest Rajasthan, India: Evidence of younger Pan-African thermal event by 40Ar-39Ar studies. Gondwana Research 2, 271-281.

Rao, C. D., Santosh, M., Kim, S. W., Li, S., 2013. Arc magmatism in the Delhi Fold Belt: SHRIMP U–Pb zircon ages of granitoids and implications for Neoproterozoic convergent margin tectonics in NW India. Journal of Asian Earth Sciences 78, 83-99.

Rasmussen, B., Bose, P. K., Sarkar, S., Banerjee, S., Fletcher, I. R., McNaughton, N. J., 2002. 1.6 Ga U-Pb zircon age for the Chorhat Sandstone, lower Vindhyan, India: Possible implications for early evolution of animals. Geology 30, 103-106.

Ray, J. S., 2006. Age of the Vindhyan Supergroup: a review of recent findings. Journal of Earth System Science 115, 149-160.

Ray, J.S., Davis, W.J., and Shukla, A.D., 2011. Age of Lower Vindhyans of Rajasthan. In Abstract volume of International Conference on Precambrian Sedimentation and Tectonics and Second GPSS Meeting, IIT Bombay, Mumbai 75.

Ray, J. S., Martin, M. W., Veizer, J., Bowring, S. A., 2002. U-Pb zircon dating and Sr isotope systematics of the Vindhyan Supergroup, India. Geology 30, 131-134.

Ray, J. S., Veizer, J., & Davis, W. J., 2003. C, O, Sr and Pb isotope systematics of carbonate sequences of the Vindhyan Supergroup, India: age, diagenesis, correlations and implications for global events. Precambrian Research 121, 103-140.

Raza, M., Casshyap, S. M., 1996. A tectono-sedimentary model of evolution of middle Proterozoic Vindhyan basin. Memoirs-Geological Society of India, 287-300.

Retallack, G. J., Matthews, N. A., Master, S., Khangar, R. G., Khan, M., 2021. Dickinsonia discovered in India and late Ediacaran biogeography. Gondwana Research 90, 165-170.

Roser, B. P., Korsch, R. J., 1988. Provenance signatures of sandstone‑mudstone suites determined using discriminant function analysis of major element data. Chemical Geology 67, 119‑139.

Sarangi, S., Gopalan, K., Kumar, S., 2004. Pb–Pb age of earliest megascopic, eukaryotic alga bearing Rohtas Formation, Vindhyan Supergroup, India: implications for Precambrian atmospheric oxygen evolution. Precambrian Research 132, 107-121.

Santos, M. M., Lana, C., Scholz, R., Buick, I., Schmitz, M. D., Kamo, S. L., Wiedenbeck, M., 2017. A new appraisal of Sri Lankan BB zircon as a reference material for LA-ICP-MS U-Pb geochronology and Lu-Hf isotope tracing. Geostandards and Geoanalytical Research 41, 335-358.

Santosh, M., Iyer, S. S., Vasconcellos, M. B. A., Enzweiler, J., 1989. Late Precambrian alkaline plutons in southwest India: geochronologic and rare-earth element constraints on Pan-African magmatism. Lithos 24, 65-79.

Santosh, M., Yokoyama, K., Biju-Sekhar, S., Rogers, J. J. W., 2003. Multiple tectonothermal events in the granulite blocks of southern India revealed from EPMA dating: implications on the history of supercontinents. Gondwana Research 6, 29-63.

Scotese, C.R., 2016. PALEOMAP PaleoAtlas for GPlates and the PaleoData Plotter Program. PALEOMAP Project. http://www.earthbyte.org/paleomap-paleoatlas-for- gplate.

Seilacher, A., Bose, P. K., Pflüger, F., 1998. Triploblastic animals more than 1 billion years ago: trace fossil evidence from India. Science 282, 80-83.

Sen, A., Pande, K., Sheth, H. C., Sharma, K. K., Sarkar, S., Dayal, A. M., Mistry, H., 2013. An

Ediacaran–Cambrian thermal imprint in Rajasthan, western India: Evidence from 40 Ar–39 Ar geochronology of the Sindreth volcanics. Journal of Earth System Science 122, 1477-1493.

Sharma, A., Das, K., Chakraborty, P. P., Shiraishi, F., & Kayama, M. (2022). U–Pb zircon geochronology of a pyroclastic rock from the Parsoi Formation, Mahakoshal Group: Implications towards age and tectonics of the Basin in Central Indian Tectonic Zone. Geological Journal.

Sharma, M., 2006. Late Palaeoproterozoic (Statherian) carbonaceous films from the Olive Shale (Koldaha Shale), Semri Group, Vindhyan Supergroup, India. Journal of the Palaeontological Society of India 51, 27-35.

Sharma, M., Shukla, Y., 2009a. Mesoproterozoic coiled megascopic fossil *Grypania spiralis* from the Rohtas Formation, Semri Group, Bihar, India. Current Science, 1636-1640.

Sharma, M., Shukla, Y., 2009b. Taxonomy and affinity of Early Mesoproterozoic megascopic helically coiled and related fossils from the Rohtas Formation, the Vindhyan Supergroup, India. Precambrian Research 173, 105-122.

Singh, S., 2020. Himalayan Magmatism through space and time. Episodes 43, 358-368.

Singh, V. K., Babu, R., Shukla, M., 2009. Discovery of carbonaceous remains from the Neoproterozoic shales of Vindhyan Supergroup, India. Journal of Evolutionary Biology Research 1, 001-017.

Sharma, M., Shukla, Y., Sergeev, V. N., 2021. Microfossils from the Krol 'A'of the Lesser Himalaya, India: Additional supporting data for its early Ediacaran age. Palaeoworld.

Sláma, J., Košler, J., Condon, D. J., Crowley, J. L., Gerdes, A., Hanchar, J. M., Whitehouse, M. J., 2008. Plešovice zircon—a new natural reference material for U–Pb and Hf isotopic microanalysis. Chemical Geology 249, 1-35.

Soni, M. K., Chakraborty, S., Jain, V. K., 1987. Vindhyan Supergroup–a review. Mem. Geol.

Soc. India, 6, 87-138.

Spencer, C. J., Kirkland, C. L., Taylor, R. J., 2016. Strategies towards statistically robust interpretations of in situ U–Pb zircon geochronology. Geoscience Frontiers 7, 581-589.

Srivastava, A. P., Rajagopalan, G., 1988. FT ages of Vindhyan glauconitic sandstone beds exposed around Rawatbhata area, Rajasthan. Journal of Geological Society of India 32, 527-529.

Srivastava, P., 2009. Trachyhystrichosphaera: An age-marker acanthomorph from the Bhander group, upper Vindhyan, Rajasthan. Journal of Earth System Science 118, 575-582.

Srivastava, P., 2012. Problematic fossils from the Palaeo-Neoproterozoic Vindhyan Supergroup, India. Arabian Journal of Geosciences 5, 1411-1422.

Srivastava, P., 2014. Largest Ediacaran discs from the Jodhpur Sandstone, Marwar Supergroup, India: their palaeontological significance. Geoscience Frontiers 5, 183-191.

Srivastava, P., Tewari, V. C., 2011. Morphological changes in microscopic–megascopic life and stromatolites recorded during Late Palaeoproterozoic–Neoproterozoic transition: the Vindhyan Supergroup, India. In Stromatolites: Interaction of Microbes with Sediments. Springer, Dordrecht 87-114.

Srivastava, P., 2002. Carbonaceous megafossils from the Dholpura Shale, uppermost Vindhyan Supergroup, Rajasthan: an age implication. Journal of Palaeontological Society of India 47, 97-105.

Stein, H. J., Hannah, J. L., Zimmerman, A., Markey, R. J., Sarkar, S. C., Pal, A. B., 2004. A 2.5 Ga porphyry Cu–Mo–Au deposit at Malanjkhand, central India: implications for Late Archean continental assembly. Precambrian Research 134, 189-226.

Tandon, S. K., Andrews, J. E., Sood, A., Mittal, S., 1998. Shrinkage and sediment supply control on multiple calcrete profile development: a case study from the Maastrichtian of Central India. Sedimentary Geology 119, 25-45.

Tandon, S. K., Andrews, J. E., 2001. Lithofacies associations and stable isotopes of palustrine and calcrete carbonates: examples from an Indian Maastrichtian regolith. Sedimentology, 48, 339-355.

Tandon, S. K., Sood, A., Andrews, J. E., Dennis, P. F., 1995. Palaeoenvironments of the dinosaur-bearing lameta beds (Maastrichtian), Narmada valley, central India. Palaeogeography, Palaeoclimatology, Palaeoecology, 117, 153-184.

Tandon, S. K., 2002. Records of the influence of Deccan volcanism on contemporary sedimentary environments in Central India. Sedimentary Geology, 147, 177-192.

Taylor, S. R., McLennan, S. M., 1985. The continental crust: its composition and evolution.

Tripathy, G. R., Singh, S. K., 2015. Re–Os depositional age for black shales from the Kaimur Group, Upper Vindhyan, India. Chemical Geology 413, 63-72.

Turner, C. C., Meert, J. G., Pandit, M. K., Kamenov, G. D., 2014. A detrital zircon U–Pb and Hf isotopic transect across the Son Valley sector of the Vindhyan Basin, India: implications for basin evolution and paleogeography. Gondwana Research 26, 348-364.

Upadhyay, D., 2008. Alkaline magmatism along the southeastern margin of the Indian shield: implications for regional geodynamics and constraints on craton–Eastern Ghats Belt suturing. Precambrian Research 162, 59-69.

Valdiya, K. S., 2016. Neoproterozoic Intracratonic Basins in Peninsular India. In The Making of India. Springer, Cham 269-297.

Van Lente, B., Ashwal, L. D., Pandit, M. K., Bowring, S. A., Torsvik, T. H., 2009. Neoproterozoic hydrothermally altered basaltic rocks from Rajasthan, northwest India: Implications for late Precambrian tectonic evolution of the Aravalli craton. Precambrian Research 170, 202-222.

Venkateshwarlu, M., Rao, J. M., 2013. Paleomagnetism of Bhander Sediments from Bhopal Inlier, Vindhyan Supergroup. Journal of the Geological Society of India 81, 330-336.

Verma, A., Shukla, U. K., 2015. Deposition of the upper Rewa sandstone formation of proterozoic Rewa group of the Vindhyan Basin, MP, India: a reappraisal. Journal of the Geological Society of India 86, 421-437.

Verma, S. K., Verma, S. P., Oliveira, E. P., Singh, V. K., Moreno, J. A., 2016. LA-SF-ICP-MS zircon U–Pb geochronology of granitic rocks from the central Bundelkhand greenstone complex, Bundelkhand craton, India. Journal of Asian Earth Sciences 118, 125-137.

Vinogradov, A.P., Tugarinov, A.I., Zhikov, C.I., Stanikova, N.I., Bibikova, E.V., Khorre, K., 1964. Geochronology of the Indian Precambrian. In: Report of the 22nd International Geological Congress, vol. 10, New Delhi 553–567.

Wang, W., Cawood, P. A., Pandit, M. K., 2021. India in the Nuna to Gondwana supercontinent cycles: Clues from the north Indian and Marwar Blocks. American Journal of Science 321(1-2), 83-117.

Wang, W., Cawood, P. A., Pandit, M. K., Zhou, M.F., Zhao, J. H., 2019. Evolving passive- and active- margin tectonics of the Paleoproterozoic Aravalli Basin, NW India. Bulletin Geological Society of America 131 (3-4), 426-443.

Wang, W., Cawood, P. A., Zhou, M. F., Pandit, M. K., Xia, X. P., Zhao, J. H., 2017. Low-δ^{18}O rhyolites from the Malani igneous suite: A positive test for South China and NW India linkage in Rodinia. Geophysical Research Letters 44(20), 10-298.

Wang, W., Pandit, M. K., Zhao, J. H., Chen, W. T., Zheng, J. P., 2018. Slab break-off triggered lithosphere-asthenosphere interaction at a convergent margin: The Neoproterozoic bimodal magmatism in NW India. Lithos 296, 281-296.

Wani, H., Mondal, M. E. A., Ahmad, I., 2022. Geochemistry of metasedimentary rocks of the Sonakhan and Mahakoshal greenstone belts, Central India: Implications for paleoweathering, paleogeography and mechanisms of greenstone belt development. Acta Geochimica 41, 64-83.

Wiedenbeck, M. A. P. C., Alle, P., Corfu, F. Y., Griffin, W. L., Meier, M., Oberli, F. V., Spiegel, W., 1995. Three natural zircon standards for U-Th-Pb, Lu-Hf, trace element and REE analyses. Geostandards newsletter 19, 1-23.

Wiedenbeck, M., Goswami, J. N., 1994. High precision 207Pb206Pb zircon geochronology using a small ion microprobe. Geochimica et Cosmochimica Acta 58, 2135-2141.

Xiao, S., Tang, Q., Hughes, N. C., McKenzie, N. R., Myrow, P. M., 2016. Biostratigraphic and detrital zircon age constraints on the basement of the Himalayan Foreland Basin: Implications for a Proterozoic link to the Lesser Himalaya and cratonic India. Terra Nova, 28, 419-426.

Xu, H., Meert, J. G., Pandit, M. K., 2022. Age of the Marwar Supergroup, NW India: A note on the U–Pb geochronology of Jodhpur Group felsic volcanics. Geoscience Frontiers 13, 101287.

Yadav, B. S., Ahmad, T., Kaulina, T., Bayanova, T., Bhutani, R., 2020. Origin of post-collisional A-type granites in the Mahakoshal Supracrustal Belt, Central Indian Tectonic Zone, India: Zircon U-Pb ages and geochemical evidences. Journal of Asian Earth Sciences 191, 104247.

List of figures

Figure 1: **(A)** Map of India showing the extent of the Vindhyan Basin, associated Bundelkhand Craton and the bounding Proterozoic mobile belts i.e., Aravalli-Delhi Fold Belt (ADFB) and Central Indian Tectonic Zone (CITZ)-Satpura Belt. **(B)** Geological map showing distribution of Precambrian and Phanerozoic rocks of Northwest and Central India with timing of granite magmatism (Adapted from Banerjee et al., 2021; Bhowmik et al., 2012; Kaur et al., 2011; de Wall et al., 2018). Numbers in white boxes represent the age of magmatic events especially the time of granite magmatism in Ga and details related to the ages are provided in the Table 1.

The dashed line shows the lineaments, fault and major shear zones. Abbreviations for the structural features are as follows: WMF = Western Margin Fault; GBF = Great Boundary Fault; SNNF = Son Narmada North Fault; SNNF = Son Narmada South Fault; GTSZ = Gavaligarh Tan Shear Zone; CIS = Central Indian Shear

Figure 2: Stratigraphic log of Vindhyan Supergroup with the proposed age constraints on the basis of geochronology and a compilation of reported zircon ages from the rocks of Vindhyan Supergroup exposed in Son Valley sector (Colleps et al., 2021; Lan et al., 2021, 2020; Turner et al., 2014) and Rajasthan sector (Malone et al., 2008; Turner et al., 2014). The superscripts represent the references used in this compilation which are as follows: 1 – Gopalan et al., 2013; 2 – Malone et al., 2008; Turner et al., 2014; 3 – Ray et al., 2003; 4 – Srivastava and Rajagopalan; 5 – Ray et al., 2011; 6 – Lan et al., 2020, 2021; 7 – Vinogradov et al., 1964; 8 – Tripathy and Singh, 2015; 9 – Gregory et al., 2006; 10 – Sarangi et al., 2004; 11 – Rasmussen et al., 2002; 12 – Ray et al., 2002; 13 – Bickford et al., 2017.

Figure 3: **(A)** Simplified Geological map of Proterozoic Vindhyan Basin showing the extent of Semri, Kaimur, Rewa and Bhander groups in Rajasthan as well as in Son Valley sector. Stars shows the location of the Ediacaran fossil bearing Upper Bhander sandstones. **(B)** Satellite image (Google Earth image) of the Bhimbetka region showing the sampling locations (22º56'40", 77º37'07"; 22º56'13.9", 77º36'42"). (C) Simplified geological map showing the sampling locations (23º09'18.8", 77º22'26"; 23º18'06", 77º21'16.6") of the Upper Bhander sandstone from Bhopal. The map is a part of Geological Quadrangle map number 56E (GSI, 1998; GQM 56E) **(D)** Field photograph of the stratigraphic horizon (Upper Bhander Sandstone) at Bhimbetka, showing sandstone and interbedded siltstone facies.

Figure 4: **(A)** Map showing the location of Jabalpur region in CITZ and in between the Maihar and Bhimbetka area. **(B)** Generalised stratigraphic chart of Jabalpur sub-region (GSI

Quadrangle map no. 55M). **(C)** Simplified local geological map of the Jabalpur and adjoining regions (part of Quadrangle map no. 55M) showing the sampling location (23º10'29.4", 79º57'48.5") and palaeocurrent direction of the younger sandstones.

Figure 5: Detailed description of Cretaceous sandstones sampled from Jabalpur for analytical studies based on new observations combined with earlier data from Tandon et al., (1995, 1998); Tandon and Andrews, (2001).

Figure 6: (A) Photomicrograph of the Upper Bhander Sandstone area under yellow line represent yellow colored siltstone lamination. **(B)** Variety of quartz grain constituting the framework mineralogy and show compact grain to grain contact with sutured boundary. **(C)** Polycrystalline quartz and overgrowth of monocrystalline quartz can be seen.

Figure 7: Chondrite-normalised REE patterns for **(A)** Upper Bhander Sanstone from Bhopal inlier and **(B)** Cretaceous Sandstones from Jabalpur. **(C)** Discriminant diagram after Roser and Korsch (1988) for the studied samples. **(D)** ICV (Cox et al., 1995) versus CIA (Nesbitt and Young, 1982) plot for the samples. **(E)** Plots of Th/Sc vs. Zr/Sc for studied samples to understand sediment recycling. **(F)** La/Sc versus Co/Th plot adopted from McLennan et al. (1993). The data for the Upper Bhander Sandstone from Maihar is taken from Banerjee and Banerjee (2010), TTG (Bundelkhand massif) from Mohan et al. (2012), Mahakoshal group of rocks from this study and Wani et al. (2022) and Madan Mahal from Yadav et al. (2020).

Figure 8: **(A)** U-Pb concordia diagram **(B)** relative probability density diagram and **(C)** Th/U ratio versus U-Pb ages plot for detrital zircons of Upper Bander Sandstone sample of Bhimbetka region. **(D)** CL images of representative zircon grains from Bhimbetka sample with their corresponding U-Pb ages (in white). Grain number is shown with yellow color.

Figure 9: **(A)** U-Pb concordia diagram **(B)** relative probability density diagram and **(C)** Th/U ratio versus U-Pb ages plot for detrital zircons of Upper Bander Sandstone sample from Bhopal region. **(D)** Combined relative probability density diagram for all Upper Bhander sandstone samples from the Bhopal inlier (Bhimbetka and around Bhopal city).

Figure 10: **(A)** Chondrite normalised REE patterns of detrital zircons from Bhimbetka sandstone. Binary diagrams of trace element concentrations and ratios for detrital zircons of Upper Bhander Sandstone at Bhimbetka **(B)** Y versus Yb/Sm **(C)** Y versus U (after Belousova et al., 2002). Numbers in figure B and C represents different types of Granitoids (1- Aplites, leucogranites; 2- granites; 3- granodiorites & tonalites).

Figure 11: Representative CL images of zircon grains from Cretaceous sandstone, with respective spot number (red) and U-Pb ages (black).

Figure 12: Probability density diagram and histogram for Jabalpur Sandstone **(A)**, Green Sandstone **(B)** and Upper Calcified Sandstone **(C)** and their corresponding U-Pb Concordia diagram (**D, E,** and **F**). Inset Th/U versus U-Pb ages for Cretaceous sandstone (G= Jabalpur Sandstone, H= Green Sandstone, and I= Upper Calcified Sandstone)

Figure 13: Comparison of detrital zircon U-Pb ages of the Cretaceous sandstone and the Upper Bhander Sandstone (Pre-Cretaceous) of Son Valley Sector (This study and compilation from Lan et al., 2020, 2021, Mckenzie et al., 2011). The lower panel represents the Pb-Pb zircon ages from the Satpura Mobile Belt (CITZ) (Adapted from Banerjee et al., 2021). The bars correspond to the Assembly ages of Gondwana - G; Rodinia - R; Columbia - C and Stabilization age of cratons - S.

Figure 14: Geological outcrop map of Indian Subcontinent adapted from Collins & Pisarevsky, 2005 and rotated into Cretaceous fit (Scotese, 2016) showing the Late Neoproterozoic-

Cambrian tectonothermal events in India. The marked ages are based on the following studies: Ashwal et al, 2013; Rathore et al., 1999; Sen et al., 2013; Dhiman & Singh, 2021; Islam et al., 1999; Majumdar & Dutta, 2016; Miller et al., 2001; Singh, 2020; Braun, 2006; Rajesh, 1996; Santosh et al., 2003; Upadhyay., 2008).

Figure 15: Palaeocontinental map showing locations of the Upper Bhander Sandstone and younger stratigraphic units of Rajasthan and Son Valley sector and their correlatable units in Lesser Himalaya. Numbers represent the locations (1– Balwan; 2 – Bhimbetka; 3 – Maihar; 4 – Nainital; 5 – Mussoorie; 6 – Pachmunda); The shades of brown represent the land area with different elevation and blue represents the shallow and deep sea. Locations are plotted on Map 88a, taken from PALAEOMAP PalaeoAtlas for GPlate (Scotese, 2016), using a rectangular projection in Gplate **(A)**. Comparison of detrital zircon geochronology and palaeobiology of the Upper Bhander and younger sequences of Rajasthan sector **(B)**, Son Valley sector **(C)** and equivalent Neoproterozoic sequences of Outer Lesser Himalaya **(D)**.

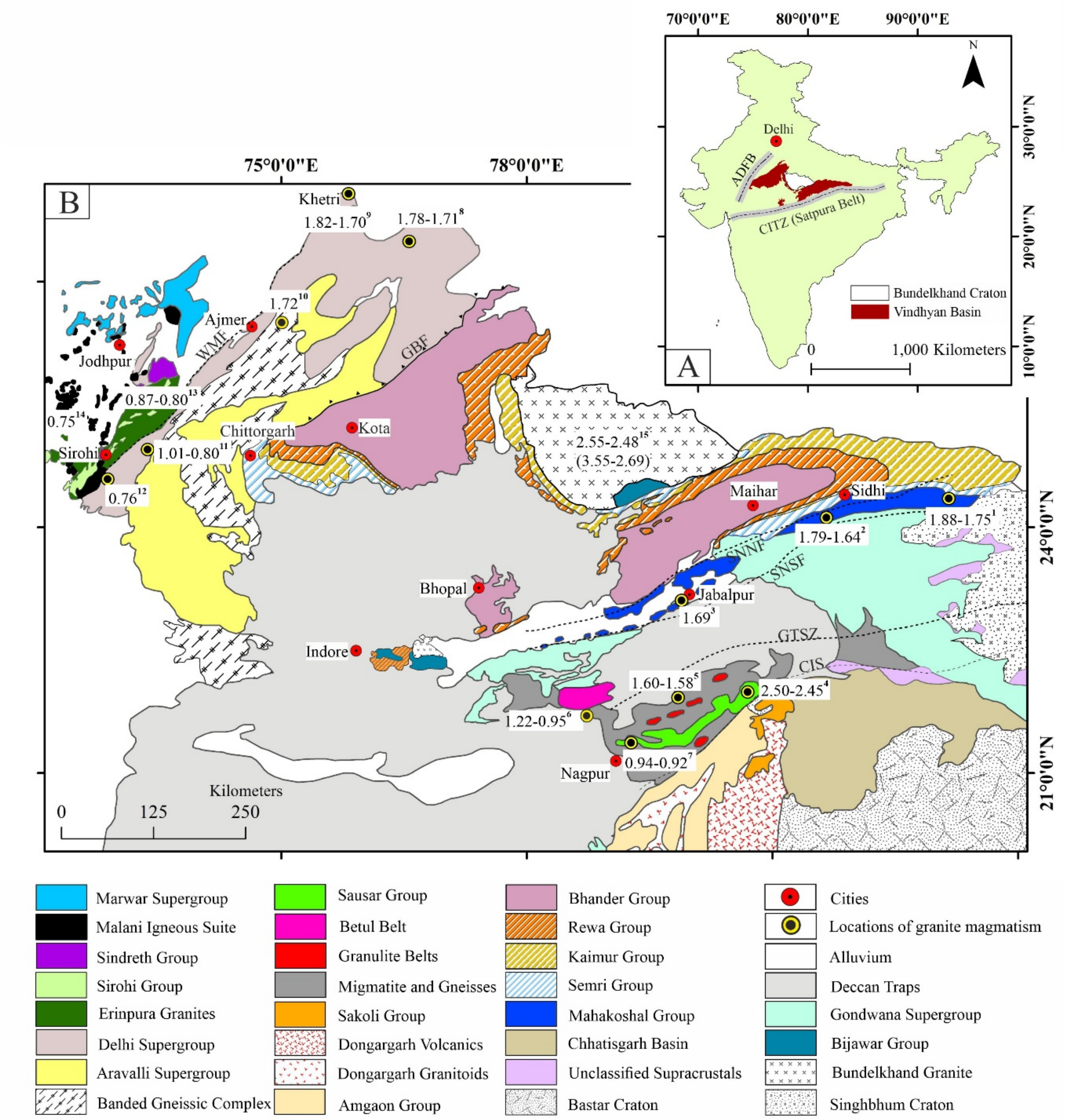

70°0'0"E
80°0'0"E
90°0'0"E
30°0'0"N
20°0'0"N
10°0'0"N
N
Delhi
ADFB
CITZ (Satpura Belt)
Bundelkhand Craton
Vindhyan Basin
0
1,000 Kilometers
A
75°0'0"E
78°0'0"E
24°0'0"N
21°0'0"N
B
Khetri
1.82-1.70
1.78-1.71
1.72
Ajmer
Jodhpur
WMF
GBF
0.87-0.80
0.75
Sirohi
1.01-0.80
0.76
Chittorgarh
Kota
2.55-2.48
(3.55-2.69)
Maihar
Sidhi
1.88-1.75
1.79-1.64
SNNF
SNSF
Bhopal
Jabalpur
1.69
Indore
GTSZ
CIS
1.60-1.58
2.50-2.45
1.22-0.95
0.94-0.92
Nagpur
Kilometers
0
125
250
Marwar Supergroup
Malani Igneous Suite
Sindreth Group
Sirohi Group
Erinpura Granites
Delhi Supergroup
Aravalli Supergroup
Banded Gneissic Complex
Sausar Group
Betul Belt
Granulite Belts
Migmatite and Gneisses
Sakoli Group
Dongargarh Volcanics
Dongargarh Granitoids
Amgaon Group
Bhander Group
Rewa Group
Kaimur Group
Semri Group
Mahakoshal Group
Chhatisgarh Basin
Unclassified Supracrustals
Bastar Craton
Cities
Locations of granite magmatism
Alluvium
Deccan Traps
Gondwana Supergroup
Bijawar Group
Bundelkhand Granite
Singhbhum Craton

Figure 1.

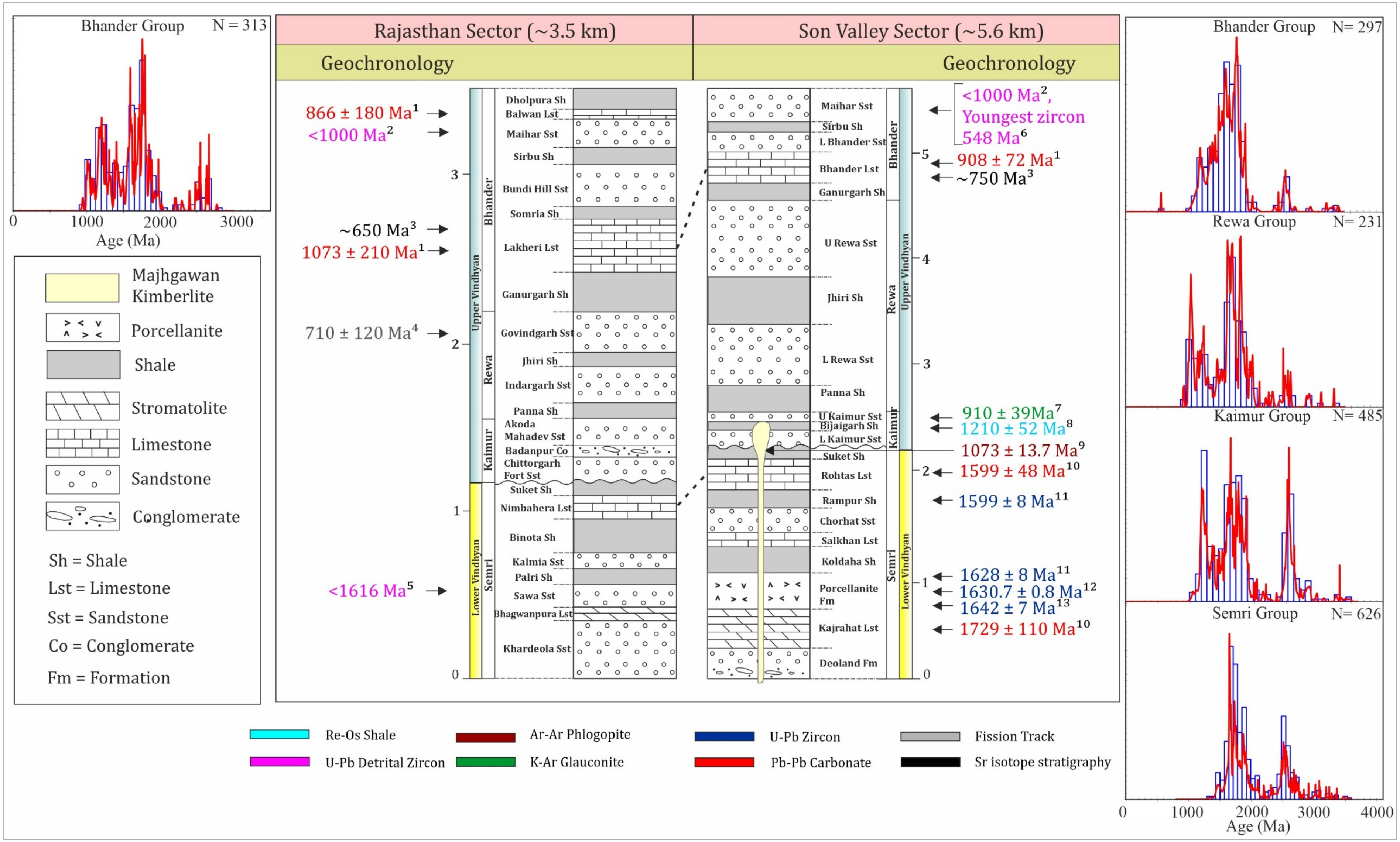
Bhander Group N = 313
Age (Ma)
Majhgawan Kimberlite
Porcellanite
Shale
Stromatolite
Limestone
Sandstone
Conglomerate
Sh = Shale
Lst = Limestone
Sst = Sandstone
Co = Conglomerate
Fm = Formation
Rajasthan Sector (~3.5 km)
Son Valley Sector (~5.6 km)
Geochronology
866 ± 180 Ma1
<1000 Ma2
~650 Ma3
1073 ± 210 Ma1
710 ± 120 Ma4
<1616 Ma5
Dholpura Sh
Balwan Lst
Maihar Sst
Sirbu Sh
Bundi Hill Sst
Somria Sh
Lakheri Lst
Ganurgarh Sh
Govindgarh Sst
Jhiri Sh
Indargarh Sst
Panna Sh
Akoda Mahadev Sst
Badanpur Co
Chittorgarh Fort Sst
Suket Sh
Nimbahera Lst
Binota Sh
Kalmia Sst
Palri Sh
Sawa Sst
Bhagwanpura Lst
Khardeola Sst
Upper Vindhyan
Lower Vindhyan
Bhander
Rewa
Kaimur
Semri
Maihar Sst
Sirbu Sh
L Bhander Sst
Bhander Lst
Ganurgarh Sh
U Rewa Sst
Jhiri Sh
L Rewa Sst
Panna Sh
U Kaimur Sst
Bijaigarh Sh
L Kaimur Sst
Suket Sh
Rohtas Lst
Rampur Sh
Chorhat Sst
Salkhan Lst
Koldaha Sh
Porcellanite Fm
Kajrahat Lst
Deoland Fm
<1000 Ma2, Youngest zircon 548 Ma6
908 ± 72 Ma1
~750 Ma3
910 ± 39Ma7
1210 ± 52 Ma8
1073 ± 13.7 Ma9
1599 ± 48 Ma10
1599 ± 8 Ma11
1628 ± 8 Ma11
1630.7 ± 0.8 Ma12
1642 ± 7 Ma13
1729 ± 110 Ma10
Bhander Group N= 297
Rewa Group N= 231
Kaimur Group N= 485
Semri Group N= 626
Age (Ma)
Re-Os Shale
U-Pb Detrital Zircon
Ar-Ar Phlogopite
K-Ar Glauconite
U-Pb Zircon
Pb-Pb Carbonate
Fission Track
Sr isotope stratigraphy

Figure 2

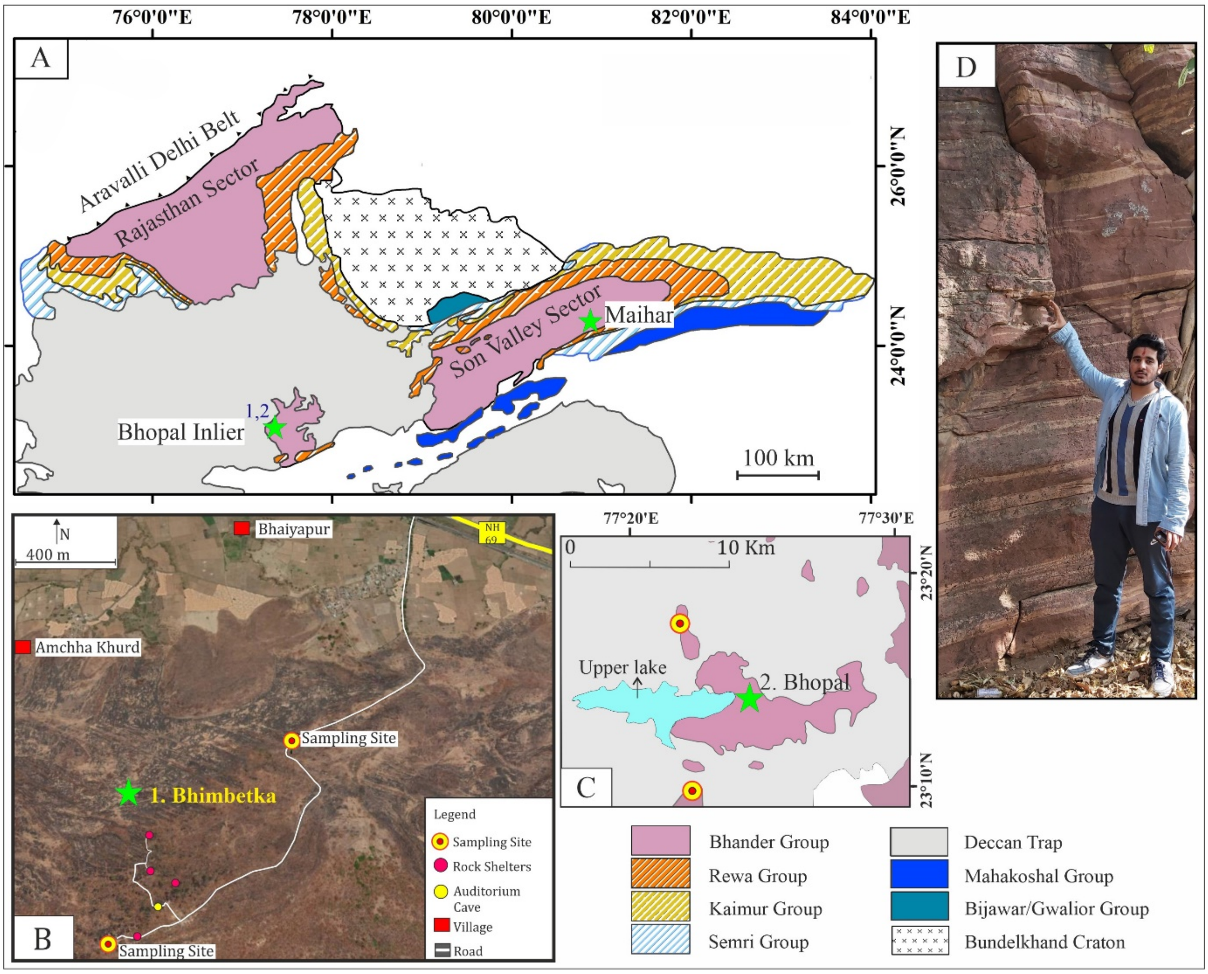

76°0'0"E
78°0'0"E
80°0'0"E
82°0'0"E
84°0'0"E
26°0'0"N
24°0'0"N
A
Aravalli Delhi Belt
Rajasthan Sector
Son Valley Sector
Maihar
1,2
Bhopal Inlier
100 km
B
N
400 m
Bhaiyapur
NH 69
Amchha Khurd
Sampling Site
1. Bhimbetka
Sampling Site
Legend
Sampling Site
Rock Shelters
Auditorium Cave
Village
Road
C
77°20'E
77°30'E
0
10 Km
23°20'N
23°10'N
Upper lake
2. Bhopal
D
Bhander Group
Rewa Group
Kaimur Group
Semri Group
Deccan Trap
Mahakoshal Group
Bijawar/Gwalior Group
Bundelkhand Craton

Figure 3.

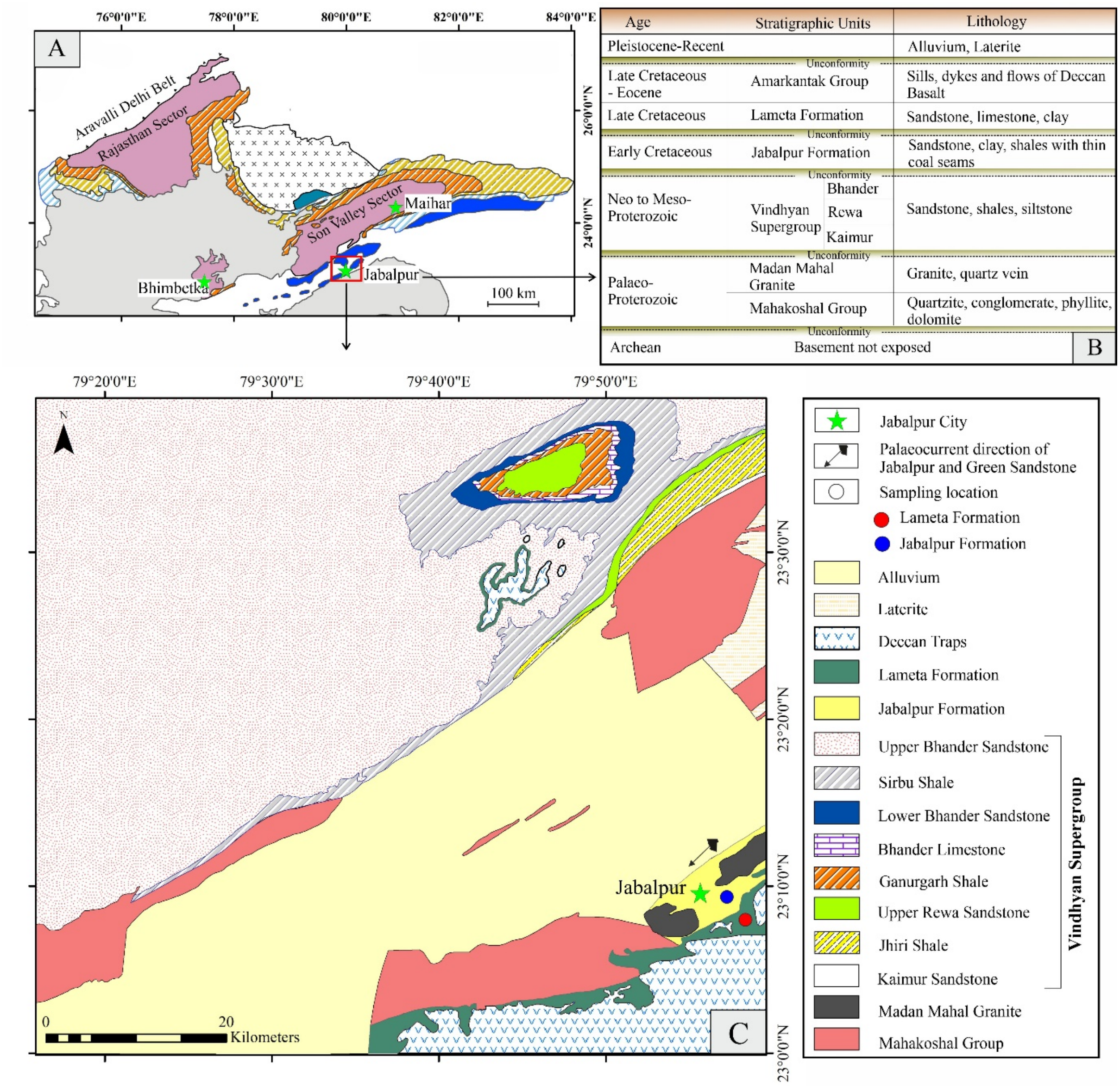
A
76°0'0"E
78°0'0"E
80°0'0"E
82°0'0"E
84°0'0"E
26°0'0"N
24°0'0"N
Aravalli Delhi Belt
Rajasthan Sector
Son Valley Sector
Maihar
Jabalpur
Bhimbetka
100 km
B
Age | Stratigraphic Units | Lithology
Pleistocene-Recent | | Alluvium, Laterite
Unconformity
Late Cretaceous - Eocene | Amarkantak Group | Sills, dykes and flows of Deccan Basalt
Late Cretaceous | Lameta Formation | Sandstone, limestone, clay
Unconformity
Early Cretaceous | Jabalpur Formation | Sandstone, clay, shales with thin coal seams
Unconformity
Neo to Meso-Proterozoic | Vindhyan Supergroup: Bhander, Rewa, Kaimur | Sandstone, shales, siltstone
Unconformity
Palaeo-Proterozoic | Madan Mahal Granite | Granite, quartz vein
Palaeo-Proterozoic | Mahakoshal Group | Quartzite, conglomerate, phyllite, dolomite
Unconformity
Archean | Basement not exposed
79°20'0"E
79°30'0"E
79°40'0"E
79°50'0"E
23°30'0"N
23°20'0"N
23°10'0"N
23°0'0"N
N
Jabalpur
0
20
Kilometers
C
Jabalpur City
Palaeocurrent direction of Jabalpur and Green Sandstone
Sampling location
Lameta Formation
Jabalpur Formation
Alluvium
Laterite
Deccan Traps
Lameta Formation
Jabalpur Formation
Upper Bhander Sandstone
Sirbu Shale
Lower Bhander Sandstone
Bhander Limestone
Ganurgarh Shale
Upper Rewa Sandstone
Jhiri Shale
Kaimur Sandstone
Madan Mahal Granite
Mahakoshal Group
Vindhyan Supergroup

Figure 4.

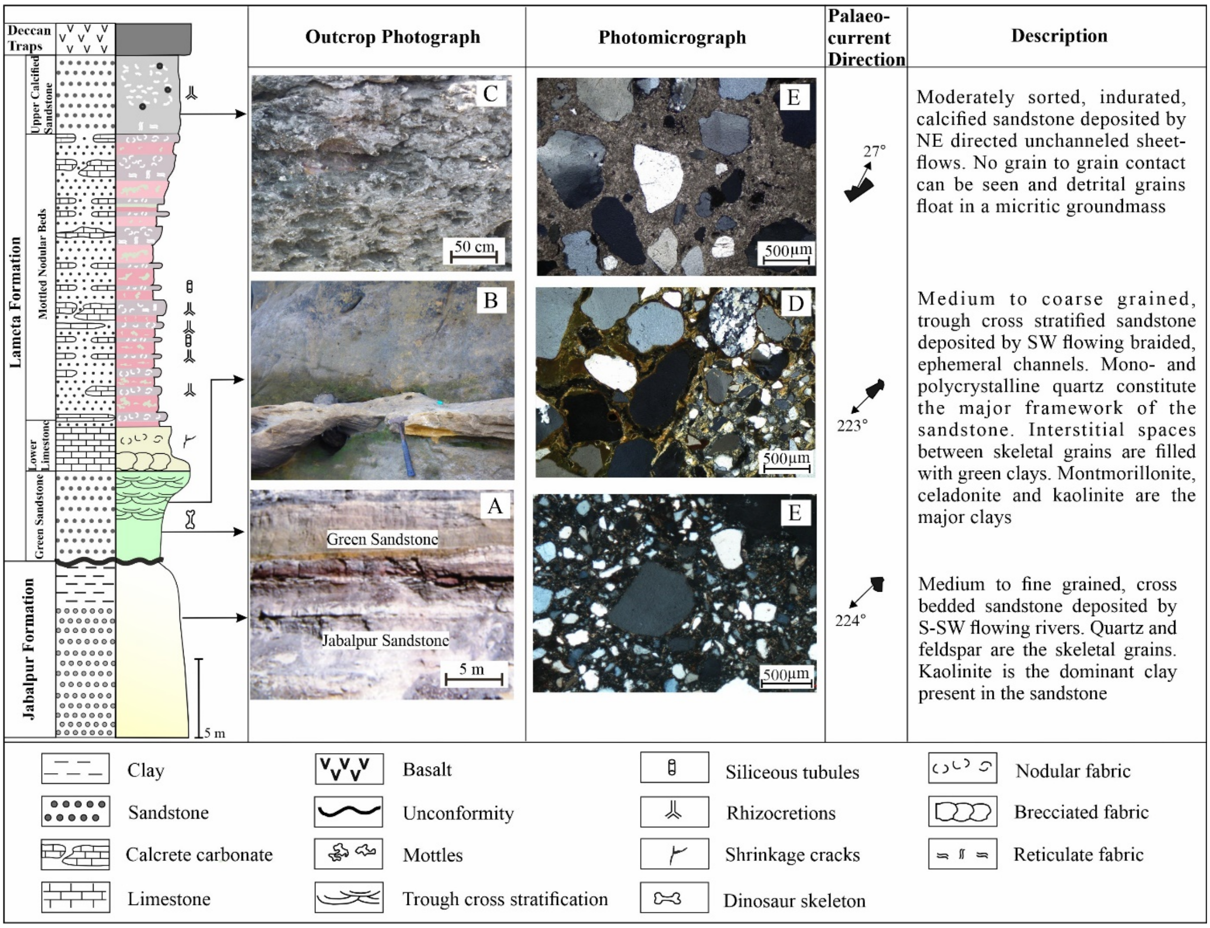
Deccan Traps
Upper Calcified Sandstone
Mottled Nodular Beds
Lameta Formation
Lower Limestone
Green Sandstone
Jabalpur Formation
5 m
Outcrop Photograph
Photomicrograph
Palaeo-current Direction
Description
C
50 cm
B
A
Green Sandstone
Jabalpur Sandstone
5 m
E
D
500μm
27°
223°
224°
Moderately sorted, indurated, calcified sandstone deposited by NE directed unchanneled sheet-flows. No grain to grain contact can be seen and detrital grains float in a micritic groundmass
Medium to coarse grained, trough cross stratified sandstone deposited by SW flowing braided, ephemeral channels. Mono- and polycrystalline quartz constitute the major framework of the sandstone. Interstitial spaces between skeletal grains are filled with green clays. Montmorillonite, celadonite and kaolinite are the major clays
Medium to fine grained, cross bedded sandstone deposited by S-SW flowing rivers. Quartz and feldspar are the skeletal grains. Kaolinite is the dominant clay present in the sandstone
Clay
Sandstone
Calcrete carbonate
Limestone
Basalt
Unconformity
Mottles
Trough cross stratification
Siliceous tubules
Rhizocretions
Shrinkage cracks
Dinosaur skeleton
Nodular fabric
Brecciated fabric
Reticulate fabric

Figure 5.

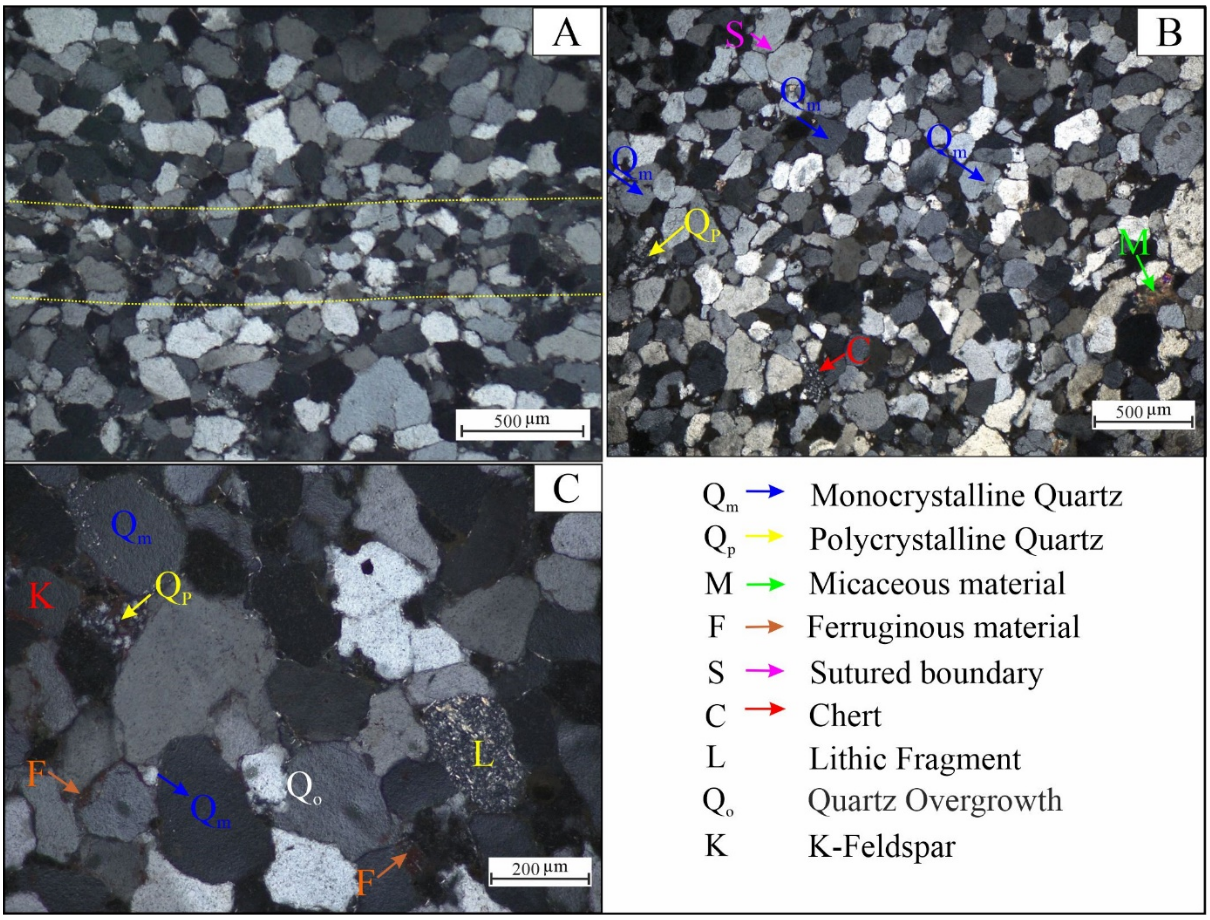
A
500 µm
B
S
Q_m
Q_m
Q_m
Q_P
M
C
500 µm
C
Q_m
K
Q_P
L
F
Q_m
Q_o
F
200 µm
Q_m Monocrystalline Quartz
Q_p Polycrystalline Quartz
M Micaceous material
F Ferruginous material
S Sutured boundary
C Chert
L Lithic Fragment
Q_o Quartz Overgrowth
K K-Feldspar

Figure 6.

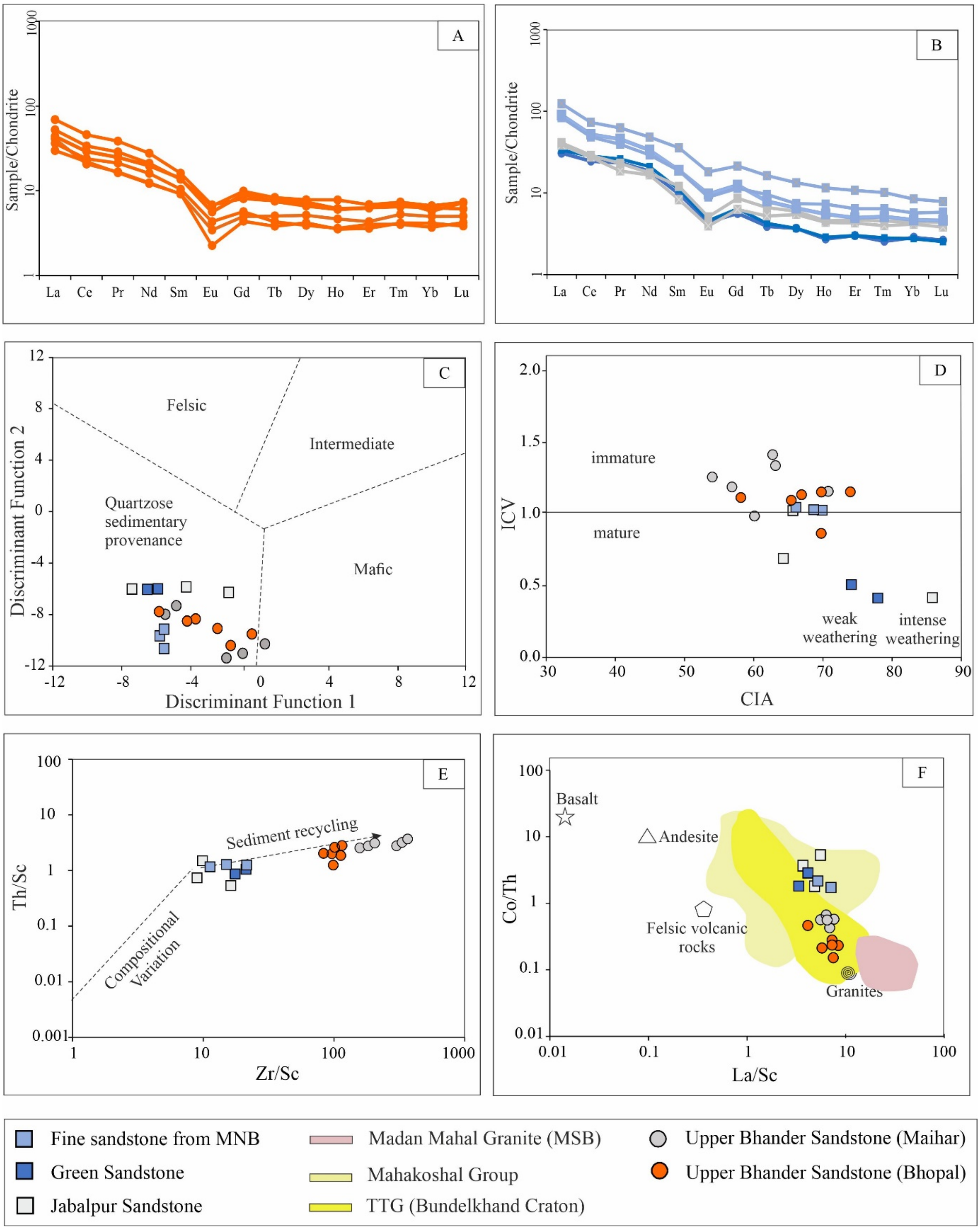
A
Sample/Chondrite
La Ce Pr Nd Sm Eu Gd Tb Dy Ho Er Tm Yb Lu
B
Sample/Chondrite
C
Felsic
Intermediate
Quartzose sedimentary provenance
Mafic
Discriminant Function 2
Discriminant Function 1
D
immature
mature
weak weathering
intense weathering
ICV
CIA
E
Sediment recycling
Compositional Variation
Th/Sc
Zr/Sc
F
Basalt
Andesite
Felsic volcanic rocks
Granites
Co/Th
La/Sc
Fine sandstone from MNB
Green Sandstone
Jabalpur Sandstone
Madan Mahal Granite (MSB)
Mahakoshal Group
TTG (Bundelkhand Craton)
Upper Bhander Sandstone (Maihar)
Upper Bhander Sandstone (Bhopal)

Figure 7.

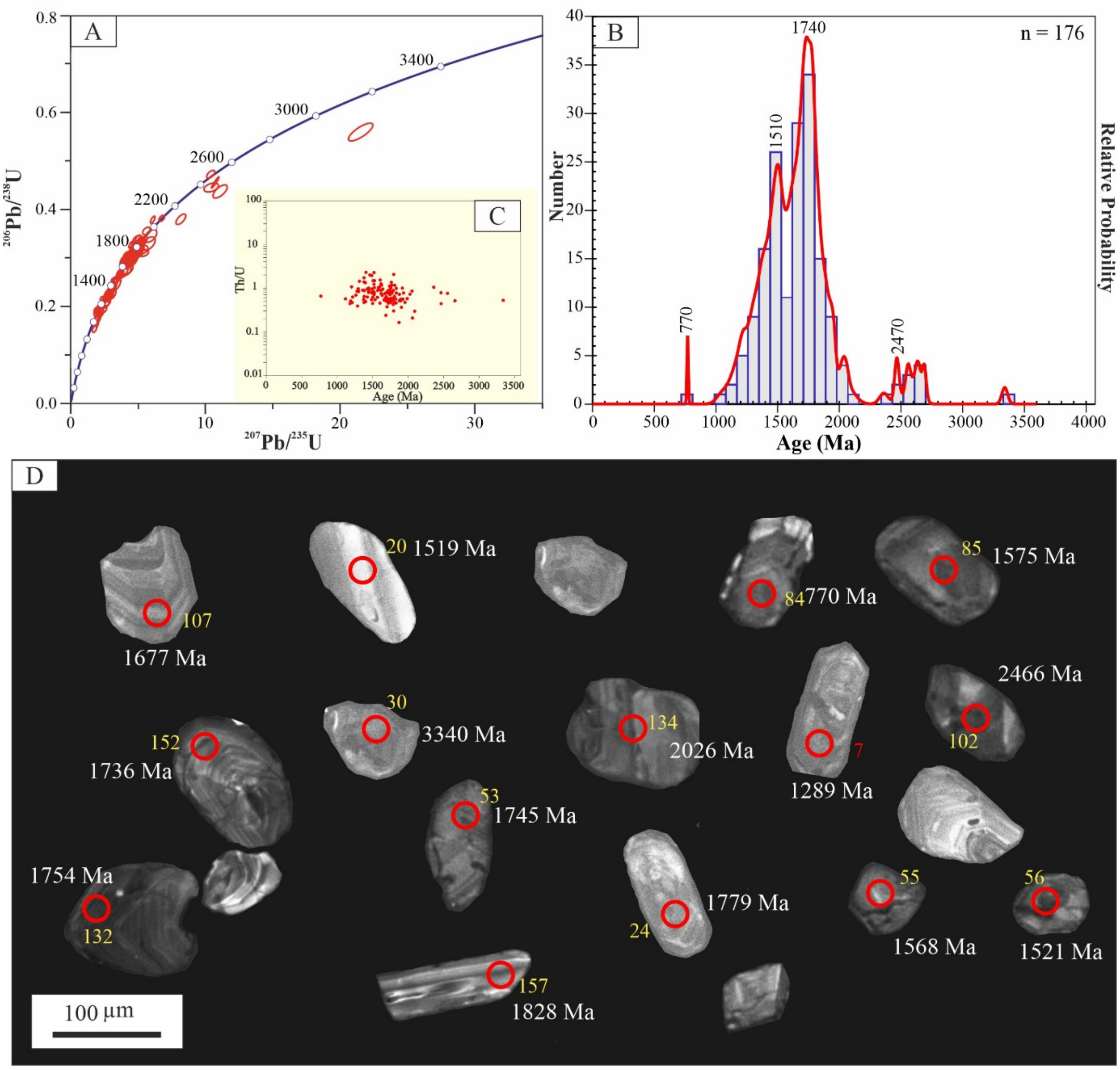
A
B
C
D
²⁰⁶Pb/²³⁸U
²⁰⁷Pb/²³⁵U
Th/U
Age (Ma)
Number
Relative Probability
n = 176
1740
1510
770
2470
3400
3000
2600
2200
1800
1400
20 1519 Ma
85 1575 Ma
107
1677 Ma
84 770 Ma
2466 Ma
30
3340 Ma
134
2026 Ma
7
1289 Ma
102
152
1736 Ma
53
1745 Ma
1754 Ma
132
1779 Ma
24
55
1568 Ma
56
1521 Ma
157
1828 Ma
100 μm

Figure 8

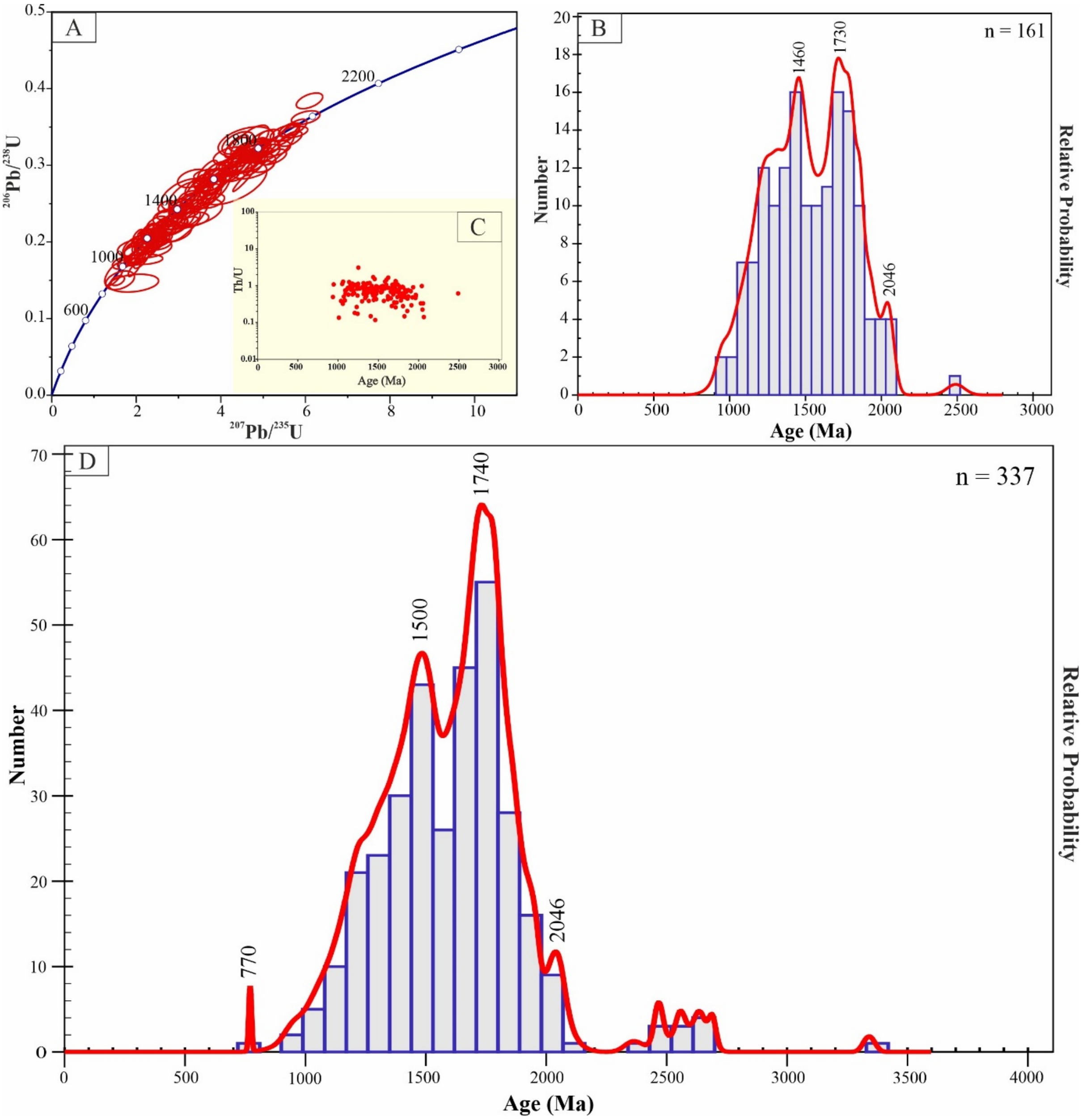
A
0.5
0.4
0.3
0.2
0.1
0.0
$^{206}Pb/^{238}U$
$^{207}Pb/^{235}U$
0
2
4
6
8
10
600
1000
1400
1800
2200
C
Th/U
Age (Ma)
B
n = 161
1460
1730
2046
Number
Relative Probability
Age (Ma)
D
n = 337
770
1500
1740
2046
Number
Relative Probability
Age (Ma)

Figure 9

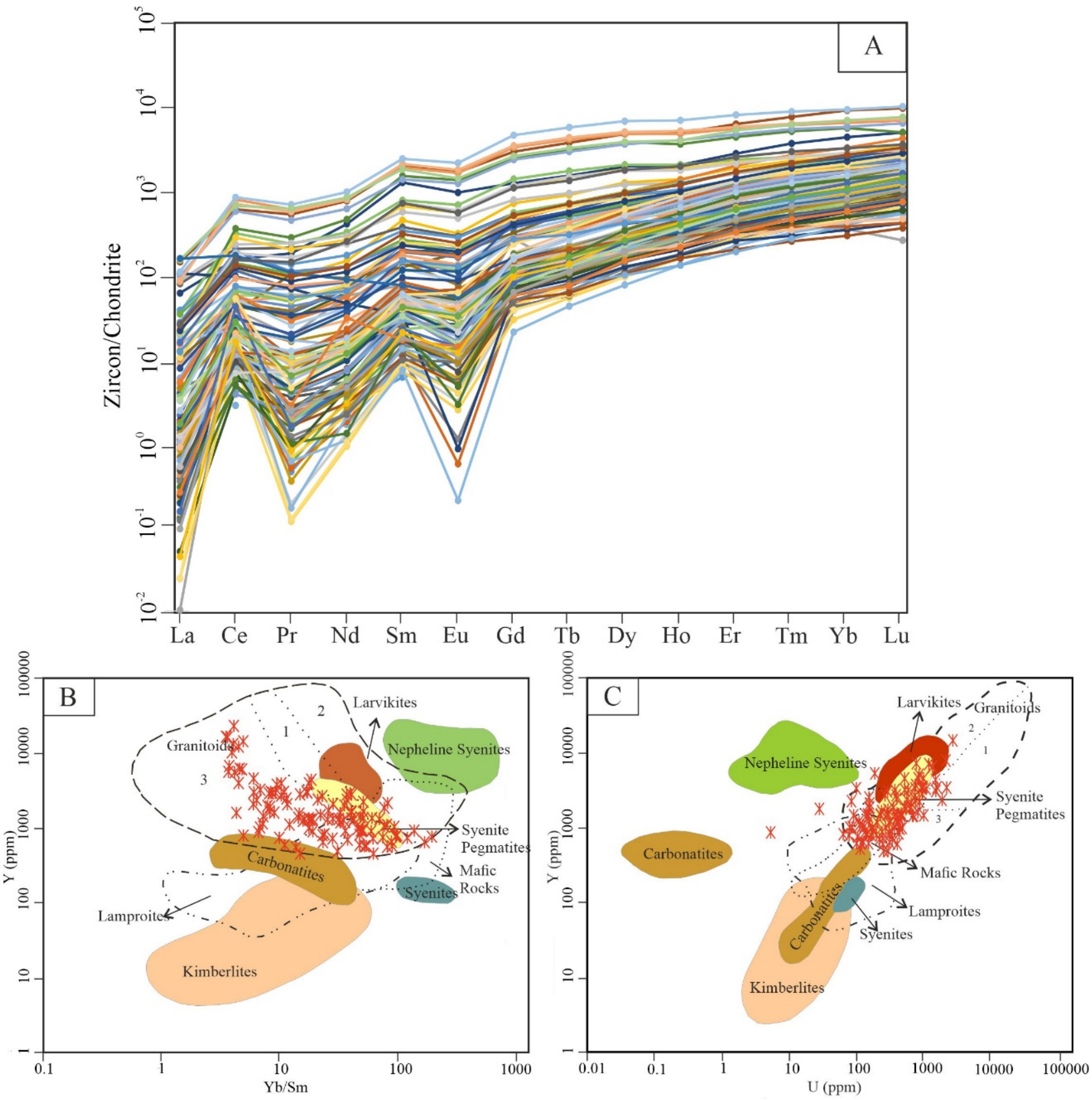
A
Zircon/Chondrite
La
Ce
Pr
Nd
Sm
Eu
Gd
Tb
Dy
Ho
Er
Tm
Yb
Lu
B
Larvikites
Granitoids
Nepheline Syenites
Syenite Pegmatites
Carbonatites
Mafic Rocks
Syenites
Lamproites
Kimberlites
Y (ppm)
Yb/Sm
C
Larvikites
Granitoids
Nepheline Syenites
Syenite Pegmatites
Carbonatites
Mafic Rocks
Lamproites
Syenites
Kimberlites
Y (ppm)
U (ppm)

Figure 10.

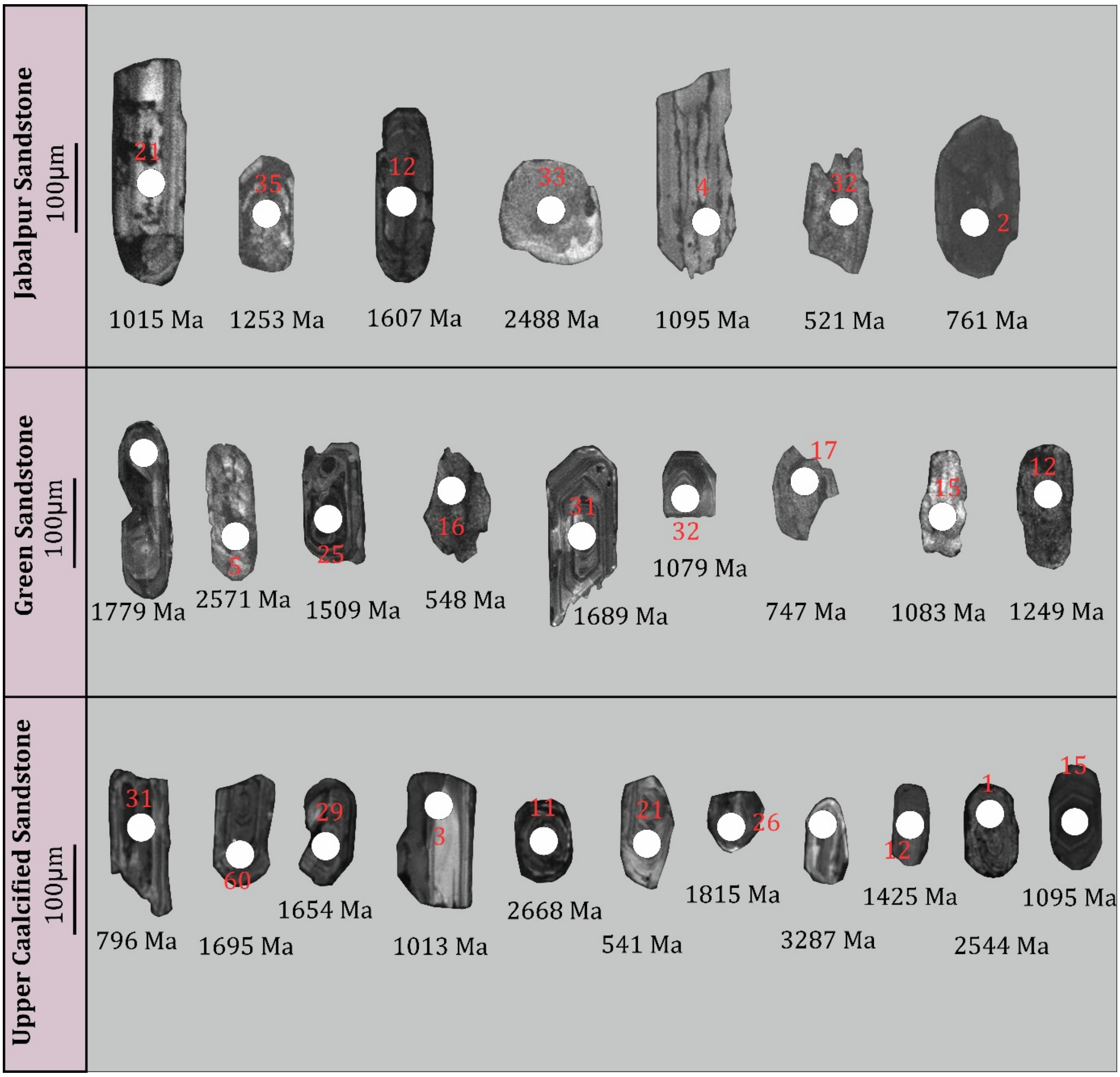
Jabalpur Sandstone
100µm
21
35
12
33
4
32
2
1015 Ma
1253 Ma
1607 Ma
2488 Ma
1095 Ma
521 Ma
761 Ma
Green Sandstone
100µm
5
25
16
31
32
17
15
12
1779 Ma
2571 Ma
1509 Ma
548 Ma
1689 Ma
1079 Ma
747 Ma
1083 Ma
1249 Ma
Upper Caalcified Sandstone
100µm
31
60
29
3
11
21
26
12
1
15
796 Ma
1695 Ma
1654 Ma
1013 Ma
2668 Ma
541 Ma
1815 Ma
3287 Ma
1425 Ma
2544 Ma
1095 Ma

Figure 11

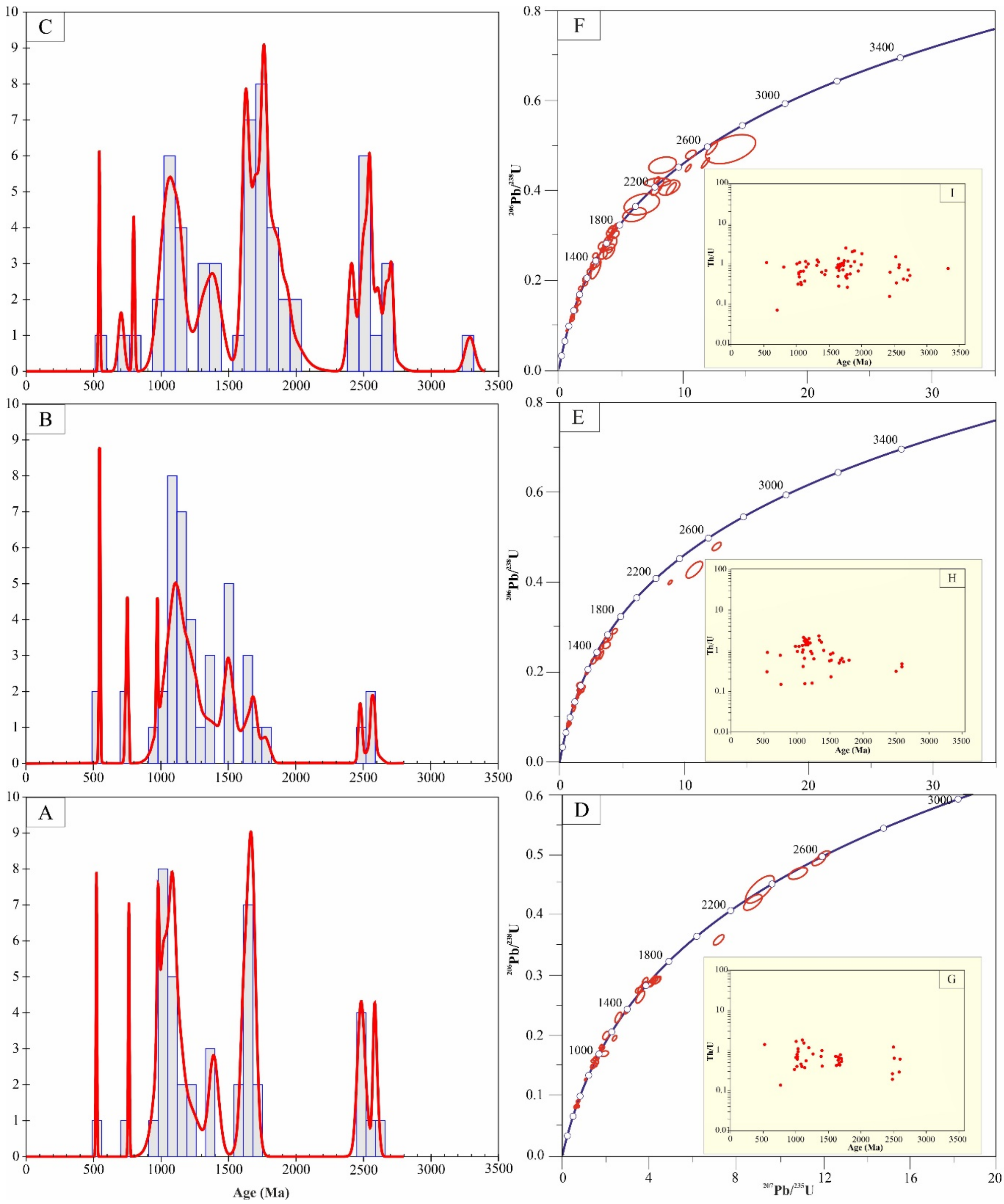

C
B
A
Age (Ma)
F
E
D
I
H
G
Th/U
Age (Ma)
$^{206}Pb/^{238}U$
$^{207}Pb/^{235}U$
1000
1400
1800
2200
2600
3000
3400

Figure 12

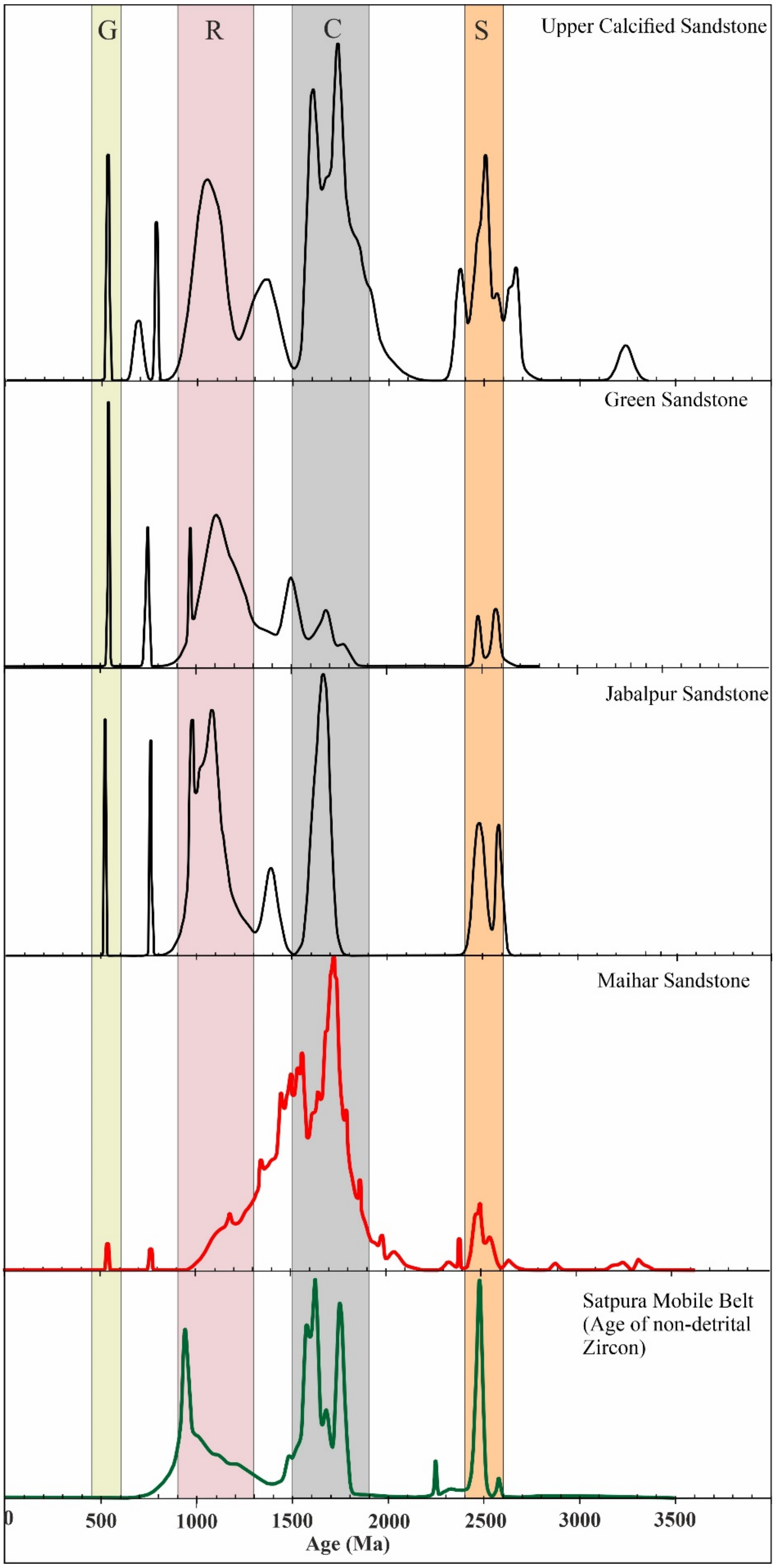
G
R
C
S
Upper Calcified Sandstone
Green Sandstone
Jabalpur Sandstone
Maihar Sandstone
Satpura Mobile Belt
(Age of non-detrital
Zircon)
0
500
1000
1500
2000
2500
3000
3500
Age (Ma)

Figure 13

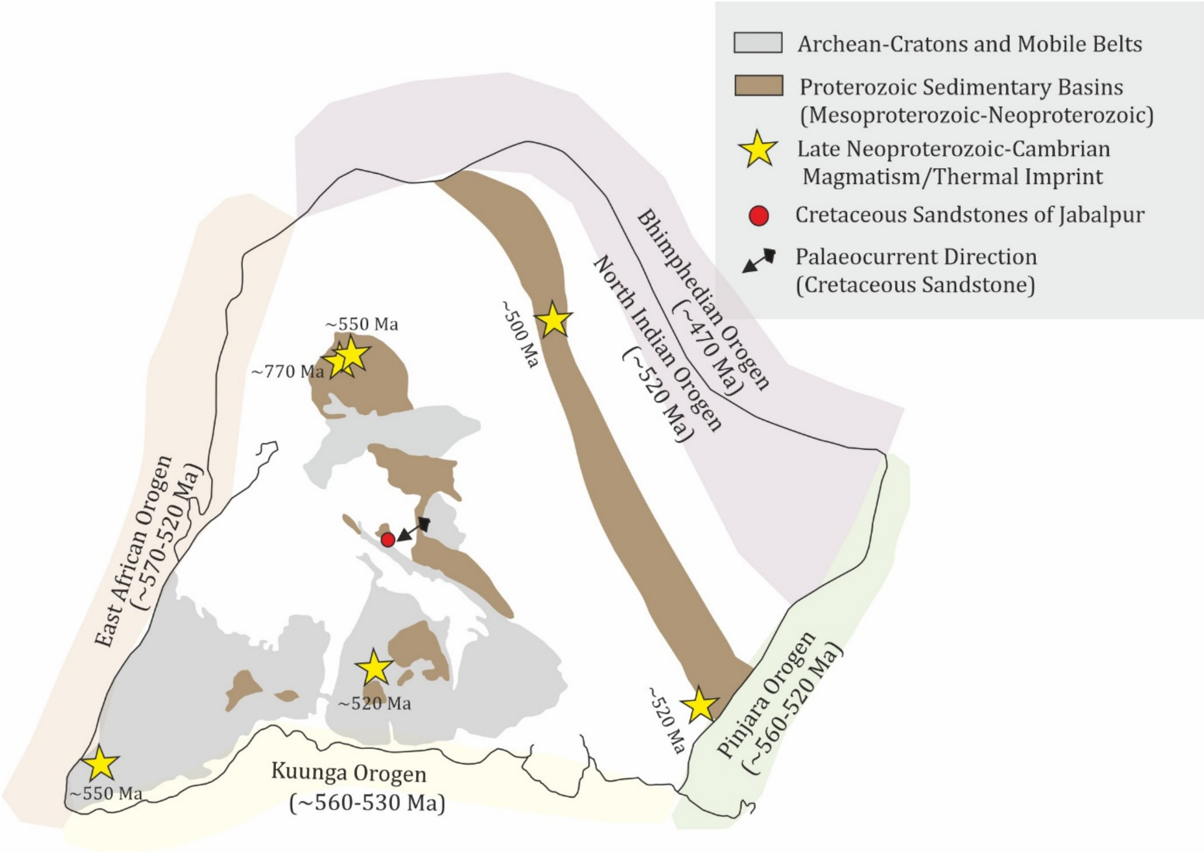
Archean-Cratons and Mobile Belts
Proterozoic Sedimentary Basins
(Mesoproterozoic-Neoproterozoic)
Late Neoproterozoic-Cambrian
Magmatism/Thermal Imprint
Cretaceous Sandstones of Jabalpur
Palaeocurrent Direction
(Cretaceous Sandstone)
Bhimphedian Orogen
(~470 Ma)
North Indian Orogen
(~520 Ma)
~500 Ma
~550 Ma
~770 Ma
East African Orogen
(~570-520 Ma)
~520 Ma
~520 Ma
Pinjara Orogen
(~560-520 Ma)
~550 Ma
Kuunga Orogen
(~560-530 Ma)

Figure 14.

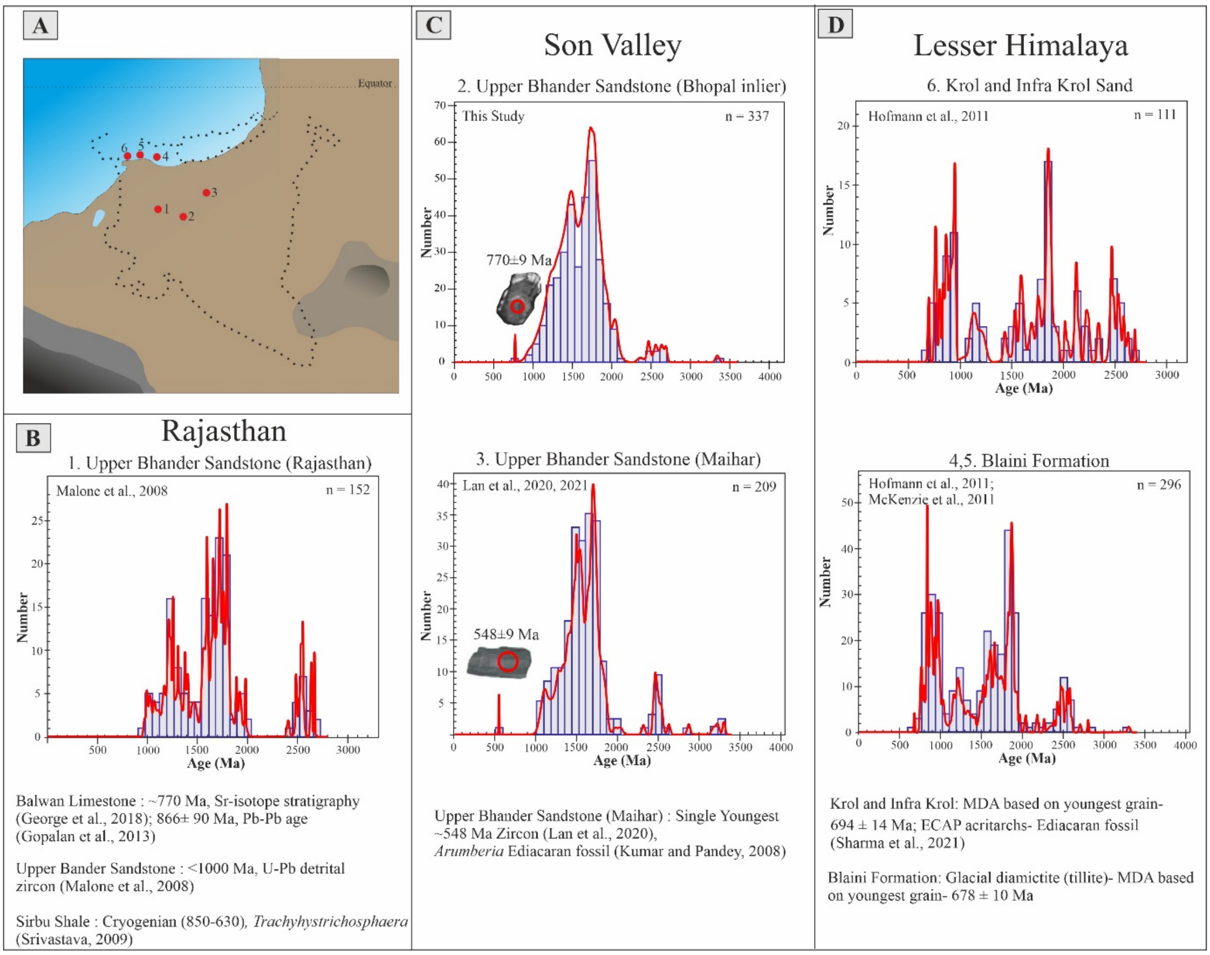

A
Equator
B
Rajasthan
1. Upper Bhander Sandstone (Rajasthan)
Malone et al., 2008
n = 152
Number
Age (Ma)
Balwan Limestone : ~770 Ma, Sr-isotope stratigraphy (George et al., 2018); 866± 90 Ma, Pb-Pb age (Gopalan et al., 2013)
Upper Bander Sandstone : <1000 Ma, U-Pb detrital zircon (Malone et al., 2008)
Sirbu Shale : Cryogenian (850-630), Trachyhystrichosphaera (Srivastava, 2009)
C
Son Valley
2. Upper Bhander Sandstone (Bhopal inlier)
This Study
n = 337
770±9 Ma
Number
3. Upper Bhander Sandstone (Maihar)
Lan et al., 2020, 2021
n = 209
548±9 Ma
Age (Ma)
Upper Bhander Sandstone (Maihar) : Single Youngest ~548 Ma Zircon (Lan et al., 2020), Arumberia Ediacaran fossil (Kumar and Pandey, 2008)
D
Lesser Himalaya
6. Krol and Infra Krol Sand
Hofmann et al., 2011
n = 111
Age (Ma)
4,5. Blaini Formation
Hofmann et al., 2011; McKenzie et al., 2011
n = 296
Krol and Infra Krol: MDA based on youngest grain- 694 ± 14 Ma; ECAP acritarchs- Ediacaran fossil (Sharma et al., 2021)
Blaini Formation: Glacial diamictite (tillite)- MDA based on youngest grain- 678 ± 10 Ma

Figure 15.

Table 1. The compilation of the magmatic events (mainly the ages of gneisses and granitoids) from the Satpura Mobile Belt (CITZ), Aravalli-BGC Craton, and Bundelkhand Craton. Numbers in bracket represent the numbers in superscripts inside the white boxes in Fig.1.

Age	Central India {CITZ (Satpura Mobile Belt)}			Noth West India (Aravalli-BGC, Aravalli Delhi Fold Belt, Sirohi and Marwar Basin)			North Central India (Bundelkhand Craton)		
	Location	**Age (Method)**	**Reference**	**Location**	**Age (Method)**	**Reference**	**Location**	**Age (Method)**	**Reference**
~500-550 Ma				Secondary thermal disturbance in Malani granite (Jalor granite)	515 ± 6 Ma (Ar-Ar age)	Rathore et al., 1999			
				Argon loss in feslic volcanics of Sindreth Basin	550–490 Ma	Sen et al., 2013			
Neoproterozoic (541-1000 Ma	Granodiorite from Sausar Group (**7**)	948 ± 4 Ma 945 Ma, (928 ± 4 Ma Post tectonic granite) (U-Th-total Pb monazite ages**)**	Chatopadhyay et al., 2015	Mirpur Granite (Malani Igneous Suite) (**14**)	753 ± 9 Ma (U – Pb Zircon TIMS)	de Wall et al., 2018			
				Mt. Abu Batholith (Sirohi terrain) (**12**)	764 ± 3 Ma, 767 ± 4 Ma (U – Pb Zircon TIMS	Ashwal et al. 2013)			
	Granitoids of Gavaligarh-Tan Shear Zone (Betul Belt) (**6**)	945±9 Ma (U-Pb zircon and U-Th-total Pb monazite ages)	Chatopadhyay et al., 2017	Erinpura Granite (Sirohi, Punagarh region) (**13**)	863 ± 23 Ma (Monazite chemical dating; 800 ± 2 and 873 ± 3 Ma (U – Pb Zircon TIMS)	Just et al., 2011; Van Lente et al., 2009			
				Sirohi terrain, Western margin of Delhi Fold Belt (**11**)	1015 ± 4, Ma, 966 ± 3 and 808 ± 3U–Pb zircon SHRIMP ages	Rao et al., 2013			

Table 1 (Continued)

Mesoproterozoic (1000-1600 Ma)	Granitoids of Gavaligarh-Tan Shear Zone (Betul Belt) (**6**)	1227±31 Ma (U-Pb zircon and U-Th-total Pb monazite ages)	Chatopadhyay et al., 2017				Quartz reef in Bundelkhand granitic massif and associated hydrothermal activity	1480 + 35 to 1660 + 40 Ma (K –Ar geochronology)	Pati et al., 1997
	Tirodi Biotite Gneiss (Sausar Belt) (**5**)	1603±23 Ma, 1584±17 Ma; (Zircon U–Pb and monazite ages)	Bhowmik et al., 2011						
Paleoproterozoic (1600-2500 Ma)	Madan Mahal Granite, Mahakoshal Belt (**3**)	1695±9 Ma Zircon U-Pb ages	Yadav et al., 2020	Granitic pluton from Alwar region (Delhi Fold Belt) (**8**)	1.78 – 1.71 Ga (Chemical dating of zircon)	Biju-Shekhar et al., 2003	Quartz reef in Bundelkhand granitic massif and associated hydrothermal activity	1790 + 40 to 1850 + 35 Ma; 1930 + 40 to 2010 + 80 Ma (K–Ar geochronology)	Pati et al., 1997
				Sakhun–Ladera region (BGC, North Central Aravalli Craton) (**10**)	1721 ± 9 Ma (U-Pb Zircon age)	Pandit et al., 2021			
	Jhirgadandi granitoids, Mahakoshal Belt (**1**)	1753±9 Ma (U–Pb SHRIMP zircon geochronology)	Bora et al., 2013, Bora and Kumar, 2015	Granitoids of Khetri copper belt (Delhi Fold Belt) (**9**)	1.82-1.70 Ga (~ 1660 Ma-Biharipur, Dabla, 1711 ± 0.5 Ma-Tehara Pluton); 1800±59 Ma, 1821.7±0.4 Ma-Jasrapur pluton (Zircon and Sm-Nd ages); 1732–1682 Ma (Zircon U-Pb and Pb-Pb ages)	Kaur et al., 2007; Kaur et al., 2009; Kaur et al., 2011)			
	Sidhi Granite, Mahakoshal Belt (**2**)	1796±17 Ma, 1645±25 Ma (Zircon U-Pb ages)	Yadav et al., 2020						

Table 1 (Continued)

				Granites and Gneisses from Pur-banera Supracrustal belt, Aravalli Craton	3159 ± 8Ma-Gneiss, 2538 ± 11Ma Granite	D'Souza et al., 2019	Central Bundelkhand greenstone complex (**15**)	Granite-2531 ± 21 Ma, 2516 ± 38 Ma, and 2514 ± 13 Ma; Gneiss-2669 ± 7.4 Ma (U-Pb Zircon ages)	Verma et al., 2016
Archean (2500-4000 Ma)	Malanjkhand Granitoids (Sausar Belt) (**4**)	2450-2500 Ma 2490±8Ma (Re–Os ages)	Stein et al., 2004	Granites (Jahazpur)	2538 ± 5 Ma (U–Pb SHRIMP zircon ages)	Dey et al., 2019	Gneisses and granites from Mahoba, Karera, Babina, Kuraichaand Panchwara, (**15**)	3.3Ga & 2.7 Ga (Gneiss); 2516±4 Ma, 2521±7 Ma (Granite); 2517±7Ma (Rhyolite) $^{207}Pb/^{206}Pb$ Zircon Ion microprobe ages	Mondal et al., 2002
				Mewar Gneiss, Aravalli Craton	3281 ± 3 Ma (small ion microprobe)	Wiedenbeck and Goswami, 1994	Gneiss from Mau Ranipur, Bundelkhand (**15**)	3551 ± 6 Ma (U–Pb and Lu-Hf isotope ages of Zircon)	Kaur et al., 2014)

Table 2. Potential sources of detritus for the Upper Bhander Sandstone at Bhimbetka.

Zircon Population	**Potential Source**	
	Proximal (From CITZ and Bundelkhand Craton)	**Distal (Aravalli BGC)**
~2.5 Ga	~2.48-2.55 Ga granitoids of Bundelkhand region, ~2.5 Ga Malanjkhand Granitoids of Sausar Belt (CITZ) (Table 1)	~2.5 Ga granitoids of Aravalli BGC (Table 1)
2000-2100 Ma	Magmatic rocks of 2.3-1.8 Ga from Chitrangi Formation of Mahakoshal Belt (CITZ) (Khanna et al., 2017)	
1650-1900 Ma	~1.88 to 1.65 Ga granitic rocks intruding the MSB (Table 1); Reworked sediments of ~1.6 Ga Deonar Porcenallintes and Rampur Shale	~1.8, 1.7–1.72 Ga magmatic rocks of Aravalli Delhi Fold Belt (Table 1)
1400-1600 Ma	1603 to 1584 Ma magmatism in Tirodi Biotite Gneiss in SMB, 1.62-1.53 Ga felsic plutonism in SMB (CITZ) (Bhowmik et al., 2014; Chattopadhyay et al., 2020); ~1534 Ma magmatic crystallization with a thermal overprint at 1454 Ma in Tirodi Gneiss (CITZ) (Ahmad et al., 2009)	
~1.0-1.1 Ga	1.05-0.95 Ga granite from the Gavilgarh-Tan Shear Zone in the CITZ; 0.94-1.06 Ga metamorphic rocks of SMB (CITZ)	Granitic intrusions of ~1.0-1.1 age from the Aravalli-BGC region and the Delhi Fold Belt (Table 1)
Ca. 770 Ma		769 to 764 Ma granites from Abu-Sirohi corridor (Table 1)

Table 3. Compilation of fossil records from Bhander Group, Son Valley sector suggesting Late Neoproterozoic age.

Formation	Fossils	Age	Reference (s)
Ganurgarh Shale	Organic-walled microfossils *(Vandalosphaeridium reticulatum, Obruchevella parva* and *Obruchevella valdaica)*	Late Cryogenian-Early Ediacaran (ca. 650-570 Ma)	Prasad et al., 2005
Nagod limestone	Organic-walled microfossils *(Obruchevella delicata*, *Obruchevella parva, Obruchevella valdaica)*	Early to Late Ediacaran	Prasad et al., 2005
Sirbu Shale	Organic-walled microfossils *(Obruchevella parva, Obruchevella delicata, CristalliniulII sp.* and *Dictyotidium sp.)*	Late Ediacaran (ca. 570-544 Ma).	Prasad et al., 2005
Bhander Limestone	Ediacara-like fossils	Ediacaran	De, 2003, 2006
Maihar Sandstone	Microbial mat structures *(Arumberia banksi* and *Rameshia rampurensis*) and Ediacaran body fossil (*Beltanelliformis minuta*) in Maihar Sandstone	Late Ediacaran	Kumar and Pandey, 2008
Nagod limestone and Sirbu Shale	Thalloid algae (multicellular metaphytes such as *Aggregatosphaera miaoheensis*, *Baculiphyca taeniata*, *Enteromorphites siniansis*)	Cryogenian to Early Ediacaran	Singh et al., 2009